



# 1 **Measurements of carbonyl compounds around the Arabian Peninsula** 2 **indicate large missing sources of acetaldehyde**

3 Nijing Wang<sup>1</sup>, Achim Edtbauer<sup>1</sup>, Christof Stöner<sup>1</sup>, Andrea Pozzer<sup>1</sup>, Efstratios Bourtsoukidis<sup>1</sup>, Lisa Ernle<sup>1</sup>,  
4 Dirk Dienhart<sup>1</sup>, Bettina Hottmann<sup>1</sup>, Horst Fischer<sup>1</sup>, Jan Schuladen<sup>1</sup>, John N. Crowley<sup>1</sup>, Jean-Daniel Paris<sup>2</sup>,  
5 Jos Lelieveld<sup>1,3</sup>, Jonathan Williams<sup>1,3</sup>

6 <sup>1</sup>Air Chemistry Department, Max Planck Institute for Chemistry, Hahn-Meitner-Weg 1, 55128 Mainz, Germany

7 <sup>2</sup>Laboratoire des Sciences du Climat et de l'Environnement, LSCE/IPSL, CEA-CNRS-UVSQ, Université Paris-Saclay, Gif-sur-  
8 Yvette, France

9 <sup>3</sup>Energy, Environment and Water Research Center, The Cyprus Institute, Nicosia, Cyprus

10 *Correspondence to:* Nijing Wang (nijing.wang@mpic.de)

## 11 **Abstract**

12 Volatile organic compounds (VOCs) were measured around the Arabian Peninsula using a research vessel during the AQABA  
13 campaign (Air Quality and Climate Change in the Arabian Basin) from June to August 2017. In this study we examine carbonyl  
14 compounds (C<sub>x</sub>H<sub>y</sub>O), measured by a proton transfer reaction mass spectrometer (PTR-ToF-MS), and present both a regional  
15 concentration distribution and a budget assessment for these key atmospheric species. Among the aliphatic carbonyls, acetone had  
16 the highest mixing ratios in most of the regions traversed, varying from 0.43 ppb over the Arabian Sea to 4.5 ppb over the Arabian  
17 Gulf, followed by formaldehyde (measured by Hantzsch monitor, 0.82 ppb over the Arabian Sea and 3.8 ppb over the Arabian  
18 Gulf) and acetaldehyde (0.16 ppb over the Arabian Sea and 1.7 ppb over the Arabian Gulf). Unsaturated carbonyls (C<sub>4</sub>-C<sub>9</sub>) varied  
19 from 10 to 700 ppt during the campaign, and followed similar regional mixing ratio dependence as aliphatic carbonyls, which were  
20 identified as oxidation products of cycloalkanes over polluted areas. An empirical method based on hydrocarbon ratios was applied  
21 to investigate the photochemical source strength of the aliphatic carbonyls. While the distribution and relative concentration  
22 enhancements of the C<sub>3</sub>-C<sub>8</sub> aliphatic carbonyls could be explained by this method, that of acetaldehyde could not. A smaller but  
23 still significant discrepancy was found when comparing measurements to global chemistry-transport model (EMAC) results, with  
24 the model underestimating the measured acetaldehyde mixing ratio up to an order of magnitude. Implementing a photolytically  
25 driven marine source of acetaldehyde significantly improved the agreement between measurements and model, particularly over  
26 the remote regions (e.g. Arabian Sea). However, the newly introduced acetaldehyde source was still insufficient to describe the  
27 observations over the most polluted regions (Arabian Gulf and Suez), where model underestimation of primary emissions and  
28 biomass burning events are possible reasons.

29

30

31

32

33

34

35



## 36 1 Introduction

37 Carbonyl compounds (aldehydes and ketones) can be released into the air directly from a variety of primary biogenic and  
38 anthropogenic sources. These include biomass burning (Holzinger et al., 1999; Holzinger et al., 2005; Koss et al., 2018), fossil fuel  
39 combustion (Reda et al., 2014; Huang et al., 2018) including vehicles (Erickson et al., 2014; Dong et al., 2014), industrial solvent  
40 use (Kim et al., 2008), and natural sources including plants and plankton (Zhou and Mopper, 1997; Warneke et al., 1999; Jacob et  
41 al., 2002; Fall, 2003; Williams et al., 2004; Bourtsoukidis et al., 2014). However, secondary production via the atmospheric  
42 oxidation of hydrocarbons is considered to be more important for many carbonyl compounds including acetone and acetaldehyde  
43 (Jacob et al., 2002; Millet et al., 2010).

44 Carbonyls have several important roles in the atmosphere. They form as stable intermediates directly after hydrocarbon oxidation  
45 by OH, O<sub>3</sub> or NO<sub>3</sub>, when the peroxy radicals initially formed react with each other (permutation reactions) or with NO. Their  
46 production is linked to tropospheric ozone formation (Carlier et al., 1986) and their loss, through oxidation and photolysis, is an  
47 important source of free radicals (HOx) in the dry upper troposphere (Colomb et al., 2006). Carbonyls serve as precursors of  
48 peroxyacetyl nitrates (PANs) which are important atmospheric NO<sub>x</sub> reservoir species (Finlayson-Pitts and Pitts, 1997; Edwards et  
49 al., 2014; Williams et al., 2000). Carbonyl compounds are also important for the growth of atmospheric particles (Kroll et al. 2005)  
50 thereby indirectly impacting the Earth's radiative balance. The atmospheric lifetimes of carbonyl compounds varies considerably,  
51 from less than one day for acetaldehyde (Millet et al., 2010) to more than 15 days for acetone (Jacob et al., 2002; Khan et al., 2015)  
52 in terms of tropospheric mean lifetime. A multiday lifetime means that carbonyl compounds can impact the air chemistry on local,  
53 regional and even hemispheric scales. The numerous primary and secondary sources of carbonyl compounds, as well as their  
54 multiple loss routes (photolysis, OH, NO<sub>3</sub> and O<sub>3</sub> oxidation) makes budget assessments difficult.

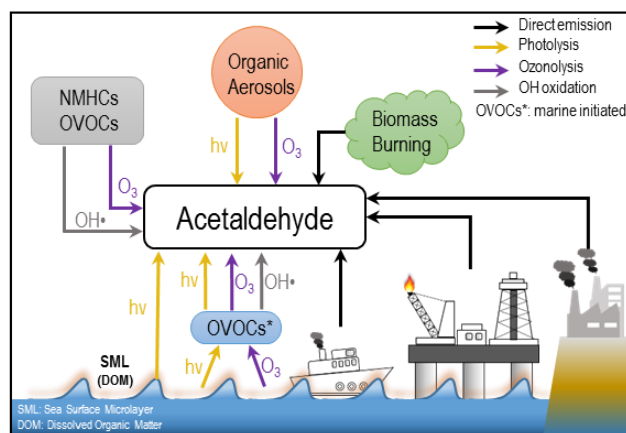
55 The most predominant atmospheric carbonyl compounds besides formaldehyde are acetaldehyde and acetone. They have been  
56 reported to vary from a few hundred ppt in remote areas (Warneke and de Gouw, 2001; Lewis et al., 2005; White et al., 2008; Colomb  
57 et al., 2009; Read et al., 2012; Sjostedt et al., 2012; Tanimoto et al., 2014; Hornbrook et al., 2016) to several ppb in urban and polluted  
58 areas (Dolgorouky et al., 2012; Guo et al., 2013; Stoekenius and McNally, 2014; Sahu et al., 2017; Sheng et al., 2018). Generally,  
59 secondary photochemical formation from various precursors is the main source in those regions. However, several recent studies  
60 have shown that acetaldehyde mixing ratios in both the remote marine boundary layer and the free troposphere could not be  
61 explained by known photochemistry as implemented in various atmospheric chemistry models, which consistently underestimated  
62 the measurements by an order of magnitude or more (Singh et al., 2003; Read et al., 2012; Wang et al., 2019). Several potential  
63 additional acetaldehyde sources have been proposed including new hydrocarbon oxidation mechanisms, aerosol related sources  
64 and oceanic sources. One possible source of acetaldehyde in the remote marine boundary layer is oceanic emission from the photo  
65 degradation of colored dissolved organic matter (CDOM) in sea-surface water, where acetaldehyde could be produced together  
66 with other low molecular weight carbonyl compounds (Kieber et al., 1990; Zhou and Mopper, 1997; Sinha et al., 2007; Dixon et al.,  
67 2013). Nevertheless, due to both limited airborne and seawater measurements of acetaldehyde, the importance of oceanic emission  
68 is still under debate (Millet et al., 2010; Wang et al., 2019). In order to better understand the atmospheric budgets of acetaldehyde  
69 (and the other carbonyl compounds), it is informative to analyze a dataset of multiple carbonyl compounds in both polluted and  
70 clean environments, with influence from marine emissions, varying particulate loadings, and high rates of oxidation as shown in  
71 Figure 1, which demonstrates the main formation pathways of acetaldehyde during this campaign.

72 During the shipborne research campaign AQABA, carbonyl compounds were continuously measured by PTR-ToF-MS onboard a  
73 research vessel that circumnavigated the Arabian Peninsula. During the campaign, chemically distinct air masses were sampled,



74 which had been influenced by primary emissions of hydrocarbons and inorganic pollutants ( $\text{NO}_x$ ,  $\text{SO}_2$  and  $\text{CO}$ ) from petroleum  
75 industries and marine transport (Bourtsoukidis et al., 2019; Celik et al., 2019), by pollution from urban areas (Pfanterstill et al.,  
76 2019), and clean marine influenced air. It is a unique dataset of carbonyl compounds encompassing starkly different environmental  
77 conditions from a region with few (or none) available in-situ measurements to date.

78 In this study, we provide an overview of carbonyl compound mixing ratios (aliphatic, unsaturated and aromatic) over the  
79 Mediterranean Sea, Suez, Red Sea, Arabian Sea and Arabian Gulf. Using an empirical method based on measured hydrocarbon  
80 precursors, we have analyzed the relative importance of the photochemical sources for the carbonyl compounds observed. The  
81 analysis is then extended to include sources and transport by using a global model EMAC (5th generation European Centre –  
82 Hamburg general circulation model, ECHAM5 coupled to the modular earth submodel system, MESSy, applied to atmospheric  
83 chemistry). Model measurement differences are investigated in both clean and polluted regions, with particular emphasis on  
84 acetaldehyde.



85  
86 Figure 1. Diagram of possible sources and formation pathways of acetaldehyde during the AQABA campaign.

87

## 88 2 Methods

### 89 2.2 AQABA campaign

90 The AQABA campaign was conducted onboard the research vessel Kommandor Iona (KI) from the end of June to the end of  
91 August 2017. The ship started from Southern France, proceeded across the Mediterranean, through the Suez Canal, around the  
92 Arabian Peninsula into the Arabian Gulf and on to Kuwait, thereafter returning along the same route. Five laboratory containers  
93 were loaded onto the vessel, containing multiple gas and particle phase measurement instruments as well as a weather station.

### 94 2.3 PTR-ToF-MS

#### 95 2.3.1 Sampling and instrument set-up

96 A high-flow inlet (stainless steel tubing, 0.2 m diameter, 5.5 m tall and 3 m above the top of the containers and the front deck) was  
97 installed at the front of the ship where the laboratory containers were located. A high flow of air (approximately  $10 \text{ m}^3 \text{ min}^{-1}$ ) was  
98 drawn through the inlet which provided a common attachment point for sub-sampling lines for all gas-phase measurement  
99 instruments. An air flow of  $5 \text{ standard L min}^{-1}$  for the first leg and  $3.5 \text{ standard L min}^{-1}$  for the second leg was pumped into the



100 VOC container through an 1/2" (O.D. = 1.27cm) FEP (fluorinated ethylene propylene) tubing (about 10 m long) insulated and heated  
101 to 50-60 °C. A PTFE (polytetrafluoroethylene) filter was placed at the beginning of the inlet to prevent insects, dust and particles  
102 entering the instruments. Every 2-5 days, the filter was replaced depending on the degree of pollution encountered. Inside the  
103 VOC instrument container, the PTR-ToF-MS (8000, Ionicon Analytik GmbH Innsbruck, Austria) sampled a sub-flow at 80-100  
104 sccm through 1/8" (0.3175 cm) FEP tubing (~ 10 m in length, insulated and heated to 60 °C) from the main fast air flow and then  
105 to the instrument's PEEK (polyether ether ketone) inlet which was likewise heated to 60 °C. The inlet system was shared with total  
106 OH reactivity measurement (Pfannerstill et al., 2019).

107 The working principle of PTR-MS has been described in detail in previous studies (Lindinger et al., 1998; Ellis and Mayhew,  
108 2013; Yuan et al., 2017). In brief, H<sub>3</sub>O<sup>+</sup> primary ions are generated in the ion source, and then drawn into the drift tube where they  
109 interact with sampled ambient air. Inside the drift tube, VOCs with a proton affinity greater than that of H<sub>2</sub>O (691 kJ mol<sup>-1</sup>) are  
110 protonated by proton transfer from H<sub>3</sub>O<sup>+</sup>. The resulting secondary ions are transferred to the detector, in this case a time-of-flight  
111 mass spectrometer with mass resolution around 3500 for the first leg and 4500 for the second leg at mass 96amu. An internal  
112 standard of trichlorobenzene (C<sub>6</sub>H<sub>3</sub>Cl<sub>3</sub>) was continuously introduced into the instrument to ensure accurate mass calibration. Every  
113 minute a spectrum with mass range (m/z) 0-450 was generated. The data reported in this study are all at 1 minute resolution unless  
114 otherwise specified.

### 115 2.3.2 Instrument characterization

116 The instrument background was determined every three hours for 10 minutes with synthetic air. 4-point calibrations were  
117 performed five times during the whole campaign using a standard gas mixture (Apel-Riemer Environmental inc., Broomfield, USA)  
118 containing 14 compounds (methanol, acetonitrile, acetaldehyde, acetone, dimethyl sulfide, isoprene, methyl vinyl ketone,  
119 methacrolein, methyl ethyl ketone, benzene, toluene, xylene, 1,3,5-trimethylbenzene and  $\alpha$ -pinene). It has been previously reported  
120 that the sensitivity of some compounds measured by PTR-MS are humidity dependent (de Gouw and Warneke, 2007). As the  
121 relative humidity (RH) was expected to be high and varying (marine boundary layer with occasional desert air influence), humidity  
122 calibration was combined with 4-point calibration by humidifying the gas mixture at different levels from 0% - 100% RH.

### 123 2.3.3 Data analysis

124 The data were initially processed by the PTR Analyzer software (Müller et al., 2013) to identify and integrate the peaks. After  
125 obtaining the raw data (counts per second for each mass identified), a custom-developed python-based program was used to further  
126 process the data to final mixing ratios. For compounds present in the standard gas cylinder, interpolated sensitivities based on the  
127 five in-campaign calibrations were applied to derive the mixing ratios; while mixing ratios of the other masses were calculated by  
128 using a proton transfer reaction rate constant ( $k_{PTR}$ ) of  $2.0 \times 10^{-9} \text{ cm}^3 \text{ s}^{-1}$ . The uncertainty associated with the mixing ratios of the  
129 calibrated compounds was around 6-17% (see Table S1). For the mixing ratios derived by assuming  $k_{PTR}$ , the accuracy was around  
130  $\pm 50\%$  (Zhao and Zhang, 2004). The detection limit (LOD) was calculated from the background measurement with 3 times the  
131 standard deviation ( $3\sigma$ ),  $52 \pm 26$  ppt for acetaldehyde,  $22 \pm 9$  ppt for acetone and  $9 \pm 6$  ppt for methyl ethyl ketone (MEK) (Table  
132 S1).

133 In this study, we have interpreted ion masses with the exact masses corresponding to C<sub>n</sub>H<sub>2n</sub>O, C<sub>n</sub>H<sub>2n-2</sub>O and C<sub>n</sub>H<sub>2n-8</sub>O as aliphatic,  
134 unsaturated and aromatic carbonyls, respectively (see exact protonated m/z in Table S2). Carbonyl compounds with a carbon  
135 number three and above can be either aldehydes or ketones, which are not distinguishable with PTR-ToF-MS using H<sub>3</sub>O<sup>+</sup> as the  
136 primary ion. However, laboratory experiments have shown that protonated aldehydic ions with carbon atoms more than three tend



137 to lose a H<sub>2</sub>O molecule and fragment to other masses (Buhr et al., 2002; Spanel et al., 2002). Moreover, although both ketones and  
138 aldehydes can be produced via atmospheric oxidation processes, ketones tend to have longer atmospheric lifetimes than aldehydes  
139 as mentioned in the introduction. Therefore, signals on the exact mass of carbonyl compounds from the PTR-ToF-MS are expected  
140 to be dominated by ketones, particularly in regions remote from the sources.

#### 141 **2.4 Meteorological data and other trace gases**

142 The meteorological data were obtained by using a commercial weather-station (Sterela) which monitored wind speed, wind  
143 direction, relative humidity (RH), temperature, speed of the vessel, and GPS etc. The actinic flux was measured by a spectral  
144 radiometer. Non methane hydrocarbons (NMHC) mixing ratios were measured by a gas chromatograph with flame ionization  
145 detector (GC-FID), for a detailed instrumental description see Bourtsoukidis et al. (2019). Formaldehyde mixing ratios were  
146 determined by a modified and optimized version of the commercially available AL4021 (Aero-Laser, Germany), which utilizes  
147 the Hantzsch technique (Stickler et al., 2006). Methane and carbon monoxide (CO) levels were monitored by a cavity ring-down  
148 spectroscopy analyzer (Picarro G2401). Ozone was measured with an absorption photometer (Model 202 Ozone Monitor, 2B  
149 Technologies, Boulder, Colorado). Due to the potential interference from sampling our own ship exhaust in which carbonyl  
150 compounds may be present (Reda et al., 2014), a filter was applied to the data set based on the wind direction and NO<sub>x</sub>, SO<sub>2</sub> and  
151 ethene levels.

#### 152 **2.5 Model simulations**

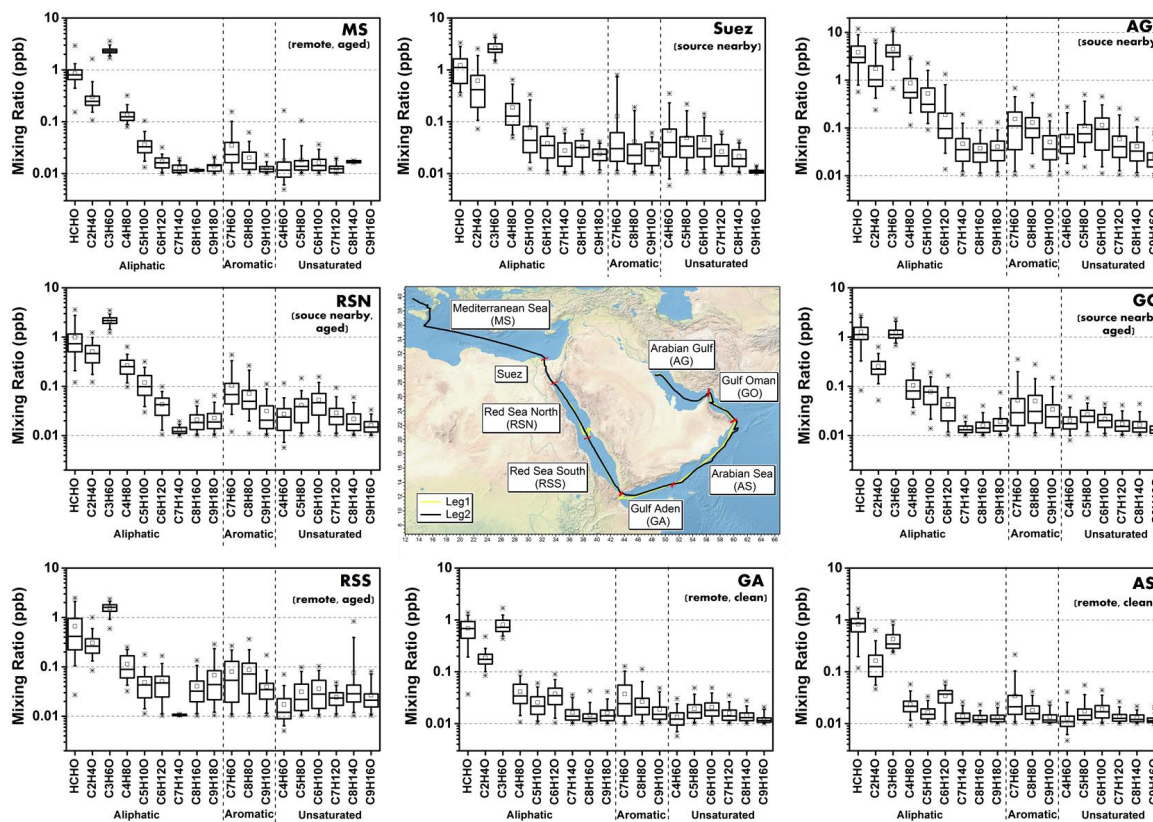
153 The EMAC (ECHAM5/MESSy Atmospheric Chemistry) model was used to simulate atmospheric mixing ratios of several  
154 carbonyl compounds along the cruise track covered during the AQABA campaign. The EMAC model is an atmospheric chemistry-  
155 general circulation model simulating the process of tropospheric air by considering processes which could influence trace gases  
156 mixing ratios, such as transport, chemistry, interaction with ocean/land, dry deposition and so on (Pozzer et al., 2007; Pozzer et al.,  
157 2012; Lelieveld et al., 2016). The model applied in this study is a combination of the 5<sup>th</sup> generation of European Centre Hamburg  
158 general circulation model (ECHAM5) (Roeckner et al., 2006) and the 2<sup>nd</sup> version of Modular Earth Submodel System (MESSy2)  
159 (Jöckel et al., 2010), where a comprehensive chemistry mechanism MOM (Mainz Organic Mechanism) was deployed (Sander et  
160 al., 2019). The model configuration in the study is the same as the model applied in Bourtsoukidis et al. (2020) in the resolution of  
161 T106L31 (i.e. ~ 1.1° × 1.1° horizontal resolution and , 31 vertical hybrid pressure levels up to 10 hPa) and the time resolution of  
162 10 minutes. The measurement data of PTR-ToF-MS were averaged to 10-minute resolution to match the model data resolution for  
163 further comparison.

### 164 **3 Results and discussion**

#### 165 **3.1 Overview of carbonyl compounds**

166 Around the Arabian Peninsula, the mixing ratios of individual carbonyl compounds varied over a wide range, from tens of ppt to  
167 ppb levels. In this study, we divided the dataset geographically into eight regions (Figure 2, middle graph) to classify and  
168 characterize the primary and secondary origins of carbonyl compounds. The regional delineations were: the Mediterranean Sea  
169 (MS), Suez, Red Sea North (RSN), Red Sea South (RSS), Gulf of Aden (GA), Arabian Sea (AS), Gulf of Oman (GO) and Arabian  
170 Gulf (AG), the same as those described by Bourtsoukidis et al. (2019). Figure 2 shows the abundance of aliphatic, aromatic and  
171 unsaturated carbonyl compounds (carbonyls) for each region. Generally, aliphatic carbonyls were present at much higher mixing  
172 ratios than aromatic and unsaturated carbonyls, with smaller carbonyl compounds (formaldehyde, acetaldehyde, C3 and C4  
173 carbonyls) dominating the distribution. The mixing ratios of aliphatic carbonyls decreased dramatically from C5 carbonyls with

174 increasing carbon number. The box plots (Figure 2) also show that carbonyl compounds were measured at higher mixing ratios  
175 and were more variable over Suez region and the Arabian Gulf. The abundance of carbonyl compounds varied markedly from  
176 region to region with highest and lowest values found in the Arabian Gulf and the Arabian Sea, respectively. Table 1 shows the  
177 mean, standard deviation and the median values for carbonyls in each region. In the following sections, each class of carbonyl  
178 compounds are investigated in greater detail.



179

180 Figure 2. Overview of mixing ratios for aliphatic, aromatic and unsaturated carbonyl compounds (CxHyO). The boxes represent  
181 25% to 75% of the data with the central line and square indicating the median and the mean values, respectively. The whiskers  
182 show data from 5% to 95% and stars were drawn for the minimum and maximum data points within 1% to 99% of the dataset.  
183 Within brackets under the region acronyms the main characteristics of the air masses are indicated, based on variability-lifetime  
184 results (b factor) from Bourtsoukidis et al. (2019) and acetone mixing ratios in this study. The data used for map plotting was from  
185 public domain GIS data found on the Natural Earth web site (<http://www.naturalearthdata.com>)  
186 and was read into Igor using the IgorGIS XOP beta.

187

188

189

190

191

192





193 Table 1. Mean, standard deviation (SD) and median mixing ratios of aliphatic, unsaturated and aromatic carbonyls in different  
194 regions.

		Aliphatic CCs								
		HCHO	CH3CHO	C3H6O	C4H8O	C5H10O	C6H12O	C7H14O	C8H16O	C9H18O
MS	mean	0.86	0.30	2.37	0.14	0.04	0.02	0.01	0.01	0.01
	SD	0.41	0.25	0.37	0.05	0.02	0.01	0.00	0.00	0.00
	median	0.80	0.25	2.32	0.12	0.03	0.02	0.01	0.01	0.01
S	mean	1.23	0.62	2.64	0.19	0.08	0.04	0.03	0.03	0.02
	SD	0.76	0.58	0.77	0.15	0.08	0.02	0.02	0.02	0.01
	median	1.11	0.42	2.52	0.13	0.04	0.04	0.02	0.03	0.02
RSN	mean	0.99	0.51	2.17	0.27	0.12	0.04	0.01	0.02	0.02
	SD	0.78	0.26	0.45	0.11	0.07	0.02	0.00	0.01	0.01
	median	0.73	0.46	2.17	0.25	0.10	0.04	0.01	0.02	0.02
RSS	mean	0.66	0.31	1.56	0.11	0.05	0.05	0.01	0.04	0.07
	SD	0.62	0.17	0.38	0.06	0.03	0.03	0.00	0.03	0.07
	median	0.40	0.26	1.60	0.09	0.04	0.05	0.01	0.03	0.04
GA	mean	0.69	0.19	0.81	0.04	0.03	0.04	0.02	0.02	0.02
	SD	0.33	0.08	0.27	0.02	0.01	0.02	0.01	0.01	0.01
	median	0.68	0.17	0.72	0.03	0.02	0.04	0.01	0.01	0.01
AS	mean	0.82	0.16	0.43	0.02	0.02	0.03	0.01	0.01	0.01
	SD	0.35	0.12	0.18	0.01	0.01	0.01	0.00	0.00	0.00
	median	0.86	0.13	0.34	0.02	0.02	0.04	0.01	0.01	0.01
GO	mean	1.27	0.26	1.33	0.10	0.08	0.04	0.01	0.02	0.02
	SD	0.59	0.12	0.40	0.06	0.04	0.03	0.00	0.01	0.01
	median	1.13	0.22	1.12	0.08	0.08	0.04	0.01	0.01	0.02
AG	mean	3.83	1.73	4.50	0.87	0.52	0.19	0.05	0.04	0.04
	SD	2.55	1.61	2.40	0.71	0.48	0.25	0.04	0.03	0.03
	median	3.02	1.02	3.77	0.56	0.31	0.10	0.04	0.03	0.03

195

196

197

198

199

200

201

202

203

204

205

206



207 Table 1. Continued

		Aromatic CCs			Unsaturated CCs					
		C7H6O	C8H8O	C9H10O	C4H6O	C5H8O	C6H10O	C7H12O	C8H14O	C9H16O
MS	mean	0.04	0.02	0.01	0.02	0.02	0.02	0.01	0.02	-
	SD	0.03	0.01	0.00	0.03	0.02	0.01	0.00	0.00	-
	median	0.02	0.02	0.01	0.01	0.01	0.01	0.01	0.02	-
S	mean	0.13	0.04	0.03	0.07	0.05	0.05	0.03	0.02	0.01
	SD	0.23	0.05	0.01	0.08	0.05	0.04	0.02	0.01	0.00
	median	0.03	0.02	0.03	0.04	0.03	0.03	0.02	0.02	0.01
RSN	mean	0.10	0.07	0.03	0.03	0.04	0.05	0.03	0.02	0.02
	SD	0.10	0.06	0.03	0.02	0.03	0.03	0.02	0.01	0.01
	median	0.07	0.05	0.02	0.02	0.04	0.05	0.02	0.02	0.02
RSS	mean	0.08	0.09	0.04	0.02	0.03	0.04	0.02	0.06	0.03
	SD	0.07	0.07	0.03	0.01	0.02	0.03	0.01	0.11	0.02
	median	0.05	0.07	0.04	0.01	0.02	0.03	0.02	0.03	0.02
GA	mean	0.04	0.03	0.02	0.01	0.02	0.02	0.02	0.01	0.01
	SD	0.03	0.02	0.01	0.01	0.01	0.01	0.01	0.00	0.00
	median	0.02	0.02	0.02	0.01	0.02	0.02	0.01	0.01	0.01
AS	mean	0.03	0.02	0.01	0.01	0.02	0.02	0.01	0.01	0.01
	SD	0.04	0.01	0.00	0.01	0.01	0.01	0.00	0.00	0.00
	median	0.02	0.02	0.01	0.01	0.01	0.02	0.01	0.01	0.01
GO	mean	0.05	0.05	0.03	0.02	0.03	0.02	0.02	0.02	0.01
	SD	0.07	0.05	0.03	0.01	0.01	0.01	0.01	0.01	0.00
	median	0.03	0.03	0.02	0.02	0.03	0.02	0.02	0.01	0.01
AG	mean	0.15	0.13	0.05	0.07	0.11	0.12	0.06	0.04	0.03
	SD	0.15	0.10	0.04	0.07	0.11	0.10	0.05	0.03	0.02
	median	0.11	0.10	0.04	0.04	0.08	0.09	0.04	0.03	0.02

208

209 **3.1.1 Aliphatic Carbonyls (C<sub>n</sub>H<sub>2n</sub>O)**

210 Relatively high mean mixing ratios of aliphatic carbonyls were observed over the Arabian Gulf; the highest being acetone (C3  
 211 carbonyl compound) at  $4.50 \pm 2.40$  ppb (median: 3.77 ppb), followed by formaldehyde at  $3.83 \pm 2.55$  ppb (median: 3.02 ppb),  
 212 acetaldehyde at  $1.73 \pm 1.61$  ppb (median: 1.02 ppb) and MEK (C4 carbonyl compound) at  $0.87 \pm 0.71$  ppb (median: 0.56 ppb).  
 213 The level of each aliphatic carbonyls over the Arabian Gulf was comparable to those previously reported for urban areas (Table  
 214 2), despite these measurements being taken at sea. As the Arabian Gulf is highly impacted by the oil and gas industry, we also  
 215 compared the measurements of the four aforementioned carbonyl compounds with those measured in the oil and gas region of the  
 216 Uinta Basin on land (Stoeckenius and McNally, 2014). Although the levels of three aliphatic carbonyls are higher in the Uinta  
 217 Basin (mean levels of 8 ppb, 4ppb and 2.8 ppb for acetone, acetaldehyde and MEK, respectively), formaldehyde was much lower  
 218 (1.9 ppb). The general distribution of the aliphatic carbonyls in the Uinta Basin is similar to the Arabian Gulf, with acetone levels  
 219 being twice as those of acetaldehyde. Koss et al. (2017) reported the max boundary layer enhancement of carbonyl compounds  
 220 (C2-C7) measured during an aircraft measurement above the most productive oil field in the United States (Permian Basin). Within  
 221 the boundary layer of the Permian Basin, C5-C7 aliphatic carbonyls had mixing ratios of 0.34 ppb, 0.08 ppb and 0.03 ppb; which





222 are of the same magnitude but lower than the levels measured over the Arabian Gulf for C5 ( $0.52 \pm 0.48$  ppb), C6 ( $0.19 \pm 0.25$ ppb)  
223 and C7 ( $0.05 \pm 0.04$  ppb) carbonyl compounds.

224 In contrast, aliphatic carbonyls had much lower average mixing ratios over the Arabian Sea and the Gulf of Aden especially for  
225 C7-C9 carbonyls with mean mixing ratios below the detection limit for most of the time. During the summertime AQABA  
226 campaign, the prevailing wind direction over the Arabian Sea was southwest (Figure S1). Four-day back trajectories indicate the  
227 air was transported from the Arabian Sea (Northwestern Indian Ocean), passing East Africa coast, which brought relatively clean,  
228 photochemically aged airmasses (Bourtsoukidis et al., 2019). The mean level of acetone over the Arabian Sea ( $0.43 \pm 0.18$  ppb,  
229 median: 0.34 ppb) is close to the level measured in the marine boundary layer of Western Indian Ocean (0.49 ppb) (Warneke and  
230 de Gouw, 2001) and comparable to other reported values from remote marine air measurement (see Table 2). Acetaldehyde was  
231 measured at relatively low mixing ratios over the Arabian Sea (median: 0.12 ppb), which is lower than the levels reported in most  
232 ground-level marine influenced sites (Lewis et al., 2005;Read et al., 2012) but comparable to the value in Barrow Alaska ( $0.10 \pm$   
233  $0.20$  ppb) (Hornbrook et al., 2016) and the values reported for Southern Indian Ocean ( $0.12 \pm 0.04$  ppb) (Colomb et al., 2009).  
234 Over the Gulf of Aden, acetone and MEK had slightly higher mixing ratios than those over the Arabian Sea.

235 The Mediterranean Sea had somewhat higher levels of aliphatic carbonyls than the clean regions (the Arabian Sea and the Gulf of  
236 Aden) but with acetone (above 2ppb) still dominating the distribution. The mean values of acetaldehyde, acetone and MEK are  
237 comparable with the results from a rural site on the west coast of Cyprus (Derstroff et al., 2017). Larger aliphatic carbonyls (C6-  
238 C9) were below the detection limit most of the time. The aliphatic carbonyls levels over the Gulf of Oman were higher than the  
239 clean regions, while C1-C5 carbonyls were more variable over the Gulf of Oman compared to those over the Mediterranean Sea.  
240 This is probably because the Gulf of Oman connects to the Arabian Gulf where intense oil and gas industrial activities are located.  
241 Over the Gulf of Oman, polluted air from the nearby sources of the Arabian Gulf is occasionally mixed with the clean air from the  
242 open sea (the Arabian Sea) under southeast wind conditions (Figure S1).

243 Another region where abundant aliphatic carbonyls were observed was Suez region. The air in this region was mainly influenced  
244 by nearby cities and marine transportation (ship emissions within the Suez Chanel) (Bourtsoukidis et al., 2019;Pfanterstill et al.,  
245 2019). However, the levels of acetaldehyde and MEK were much less compared to the levels reported from urban sites (see Table  
246 2). Interestingly, the mean acetaldehyde mixing ratio ( $0.62 \pm 0.59$  ppb) over Suez was twice the level found over the Mediterranean  
247 Sea, whilst the acetone level was only slightly higher. Besides the local-scale emission and photochemical production contribution  
248 to the acetone over Suez, the longer lived acetone could be also transported from the Mediterranean Sea (where acetone was high).  
249 Although the mean mixing ratios of aliphatic carbonyls over Suez were lower than those over the Arabian Gulf, larger variations  
250 were observed.

251 Over the Red Sea, acetone was the most abundant aliphatic carbonyls followed by formaldehyde and acetaldehyde. The mixing  
252 ratios of aliphatic C2-C4 carbonyls over the northern part of the Red Sea were similar to those levels measured in Thompson Farm  
253 (a rural site in the US, Table 2). It is worth noticing that the levels of aliphatic carbonyls in the northern part of the Red Sea were  
254 almost two times higher than the southern part of the Red Sea. According to the four-day back trajectories reported by  
255 Bourtsoukidis et al. (2019), the measured air masses travelled to the northern part was from southern Europe and northeast Africa  
256 while the southern part was more influenced by the air from the northern part Red Sea mixed with the air masses from desertic  
257 areas of central Africa. Therefore, the higher carbonyl mixing ratios over the northern part Red Sea could be due to sources of  
258 carbonyl precursors nearby and also the influence of aged air from over the Mediterranean Sea and polluted air from Suez region.

259



260 Table 2. Reported mixing ratios (ppb) of OVOCs

Location	Time	Technique	Acetaldehyde	Acetone	MEK	HCHO	Literature
<b>Marine (Sea)</b>							
Mace Head, Ireland	Jul.-Sep.	GC-FID	0.44 (0.12-2.12)	0.50 (0.16-1.67)	n.r.	n.r.	(Lewis et al., 2005)
Appledore Island, USA	Jul.-Aug.	PTR-MS	0.40	1.5	0.20	n.r.	(White et al., 2008)
Western North Pacific Ocean	May	PTR-MS	n.r.	0.20-0.70	n.r.	n.r.	(Tanimoto et al., 2014)
Canadian Archipelago	Aug.-Sep.	PTR-MS	n.r.	0.34 <sup>a</sup>	n.r.	n.r.	(Sjostedt et al., 2012)
Western Indian Ocean	Feb.-Mar.	PTR-MS	n.r.	0.49	n.r.	n.r.	(Warneke and de Gouw, 2001)
Cape Verde Atmospheric Observatory	2006-2011	GC-FID	0.43 (0.19-0.67)	0.55 (0.23-0.91)	n.r.	n.r.	(Read et al., 2012)
Barrow Arctic, Alaska	Springtime 2009	TOGA	0.10 ± 0.20	0.90 ± 0.30	0.19 ± 0.05	n.r.	(Hornbrook et al., 2016)
Southern Indian Ocean	Dec. 2004	PTR-MS	0.12 - 0.52	0.42 - 1.08	n.r.	n.r.	(Colomb et al., 2009)
<b>Urban</b>							
Paris	Jan.- Feb.	PTR-MS/ GC-MS	1.87 (0.92-4.49)	1.05 (0.58-2.97)	n.r.	n.r.	(Dolgorouky et al., 2012)
Hong Kong	Sep.-Nov.	HPLC	2.17 <sup>b</sup>	n.r.	n.r.	2.93 <sup>b</sup>	(Guo et al., 2013)
Ahmedabad	Mar.	PTR-ToF-MS	4.84 (2.74-9.86)	5.63 (3.12-12.9)	n.r.	n.r.	(Sahu et al., 2017)
Beijing	Winter (clear day)	PTR-ToF-MS	4.37	2.22	2.53	18.32	(Sheng et al., 2018)
<b>Oil &amp; Gas region</b>							
Uintah Basin, USA	2013	PTR-MS	4.0	8.0	2.8	1.9	(Stoeckenius and McNally, 2014)
<b>Rural</b>							
Thompson Farm, USA	Long-term (Summer)	PTR-MS	0.54 (0.21-1.27)	2.11 (0.98-4.08)	0.22 (0.08-0.60)	n.r.	(Jordan et al., 2009)
Cyprian rural site	Jul.-Aug.	PTR-ToF-MS	0.29 <sup>a</sup>	2.4 <sup>a</sup>	0.10 <sup>a</sup>		(Derstroff et al., 2017)
<b>Forest</b>							
Brazilian mixed tropical rainforest site	Feb.- Oct.	PTR-MS	n.r.	n.r.	0.13 <sup>c</sup>	n.r.	(Yáñez-Serrano et al., 2016)

n.r.: not reported in the literature.

<sup>a</sup> Averaged value of reported values in the literature.

<sup>b</sup> converted from values in unit of  $\mu\text{g m}^{-3}$  in the literature

<sup>c</sup> daytime average

261

262

263

264

265

266



### 267 3.1.2 Unsaturated and aromatic carbonyls ( $C_nH_{2n-2}O$ ), ( $C_nH_{2n-8}O$ )

268 The mixing ratios of unsaturated carbonyls were generally low with values below 30 ppt over the Mediterranean Sea and the clean  
269 regions (the Arabian Sea and the Gulf of Aden, 12 - 21 ppt). The Red Sea region and the Gulf of Oman had slightly higher levels  
270 (13 – 60 ppt). The highest values were again observed in the Arabian Gulf (25 – 115 ppt) followed by Suez (11 – 68 ppt). In terms  
271 of the mixing ratio distribution (Figure 2), the peak value was usually observed at C5 or C6 unsaturated carbonyls over most  
272 regions except for Suez where C4 carbonyl had the highest mixing ratio. Based on chemical formulas, unsaturated carbonyls can  
273 be either cyclic carbonyl compounds or carbonyls containing a carbon-carbon double bond. Therefore, the air chemistry could  
274 differ considerably depending on the compound assignment. A detailed analysis of the chemistry of the unsaturated carbonyls  
275 measured will be given in the following section 3.2.2.

276 Regional variability was also observed for aromatic carbonyls with highest levels observed over the Arabian Gulf and Suez, and  
277 much lower mixing ratios over the Arabian Sea, Mediterranean Sea and Gulf of Aden (Table 1). Several studies using PTR-MS  
278 have reported values for  $m/z$  107.049 (C7 aromatic carbonyls) attributed to benzaldehyde (Brilli et al., 2014; Koss et al., 2017; Koss  
279 et al., 2018),  $m/z$  121.065 (C8 aromatic carbonyls) attributed to tolualdehyde (Koss et al., 2018) or acetophenone (Brilli et al.,  
280 2014) and  $m/z$  135.080 (C9 aromatic carbonyls) attributed to methyl acetophenone (Koss et al., 2018) or benzyl methyl ketone  
281 (Brilli et al., 2014) or 3,5-dimethylbenzaldehyde (Müller et al., 2012). Atmospheric aromatic carbonyls are produced via  
282 photochemical oxidation of aromatic hydrocarbons (Finlayson-Pitts and Pitts Jr, 1999; Wyche et al., 2009; Müller et al., 2012) and  
283 benzaldehyde was reported as having primary sources from biomass burning and anthropogenic emissions (Cabrera-Perez et al.,  
284 2016). Around the Arabian Peninsula, the level of aromatic carbonyls declined with increasing carbon number over most of the  
285 regions except in the Red Sea South where C8 carbonyls were slightly higher than C7 (Figure 2). Interestingly, only in the Suez  
286 region, were the C7 aromatic carbonyls more abundant than other aromatic carbonyls, whereby the mean value ( $128 \pm 229$  ppt)  
287 was much higher than the median value (30 ppt), indicating strong primary sources of benzaldehyde in Suez. Otherwise, toluene  
288 was found to be more abundant over Suez with mean mixing ratios of  $271 \pm 459$  ppt than over other regions (the mean over the  
289 Arabian Gulf:  $130 \pm 160$  ppt) which would also lead to higher benzaldehyde as it is one of the OH-induced oxidation products of  
290 toluene via H-abstraction (Ji et al., 2017).

## 291 3.2 Chemistry of aliphatic carbonyls

### 292 3.2.1 Importance of OH photochemistry

293 Aliphatic Carbonyls are a major fraction of all oxygenated volatile organic compounds (OVOCs) in the atmosphere. They can be  
294 directly emitted into the atmosphere; however, secondary production via photo oxidation of hydrocarbons is considered as the  
295 dominant atmospheric source. In order to better understand the contribution of hydrocarbon oxidation to aliphatic carbonyls in the  
296 AQABA region, we performed empirical calculations based on the measured precursor hydrocarbon levels to estimate secondary  
297 produced aliphatic carbonyls. Subsequently, we compared the calculated values with the measured levels of the aliphatic carbonyls.  
298 The calculations are based on the following assumptions: (1) the production and the sinks of aliphatic carbonyls are governed by  
299 OH radicals; (2) primary sources of aliphatic carbonyls are insignificant; (3) only methane and 11 other measured hydrocarbon  
300 species (Table S4) reported by (Bourtsoukidis et al., 2019) were considered in the calculation. The concentration of each aliphatic  
301 carbonyl can be calculated as follows:

$$302 [HC]_{initial} = [HC] / \exp(-k_{OH+HC}[OH]\Delta t) \quad \text{Eq. (1)}$$

$$303 [Aliphatic\ carbonyls]_i = \sum([HC]_{initial} \cdot (1 - \exp(-k_{OH+HC}[OH]\Delta t) \cdot Y) \cdot \exp(-k_{OH+Aliphatic\ carbonyls}[OH]\Delta t)) \quad \text{Eq. (2)}$$



304  $[HC]_{initial}$  represents the initial mixing ratios of hydrocarbons from the source, which could be calculated using equation (1),  
305 where  $[HC]$  stands for the mean mixing ratios of measured hydrocarbons. The parameters  $k_{OH+NMHC}$  (equation 1 and 2) and  
306  $k_{OH+Aliphatic\ carbonyls}$  (equation 2) are the rate constants for the reaction between the OH radical and the corresponding  
307 hydrocarbon and aliphatic carbonyl (see Table S3). For carbonyls with a carbon number larger than four, an average reaction rate  
308 constant for the possible isomeric ketones was used since the exact structure is not known. Y is the yield of aliphatic carbonyls  
309 produced in hydrocarbon oxidation, derived from the Master Chemical Mechanism, MCM v3.2 via website:  
310 <http://mcm.leeds.ac.uk/MCM> (last accessed on Jan-15, 2020) (Jenkin et al., 1997;Saunders et al., 2003). The yields (Table S4)  
311 were determined assuming that the oxidation is dominated by OH chemistry and that alkylperoxy radicals ( $RO_2$ ) mainly react with  
312 NO. The OH exposure term  $[OH]\Delta t$  in both equations was derived from a method based on hydrocarbon ratios (Roberts et al.,  
313 1984;de Gouw et al., 2005;Yuan et al., 2012), and was calculated using the following equation:

$$314 \quad [OH]\Delta t = \frac{1}{k_X - k_Y} \cdot \left( \ln \frac{[X]}{[Y]} \Big|_{t=0} - \ln \frac{[X]}{[Y]} \right), \quad \text{Eq. (3)}$$

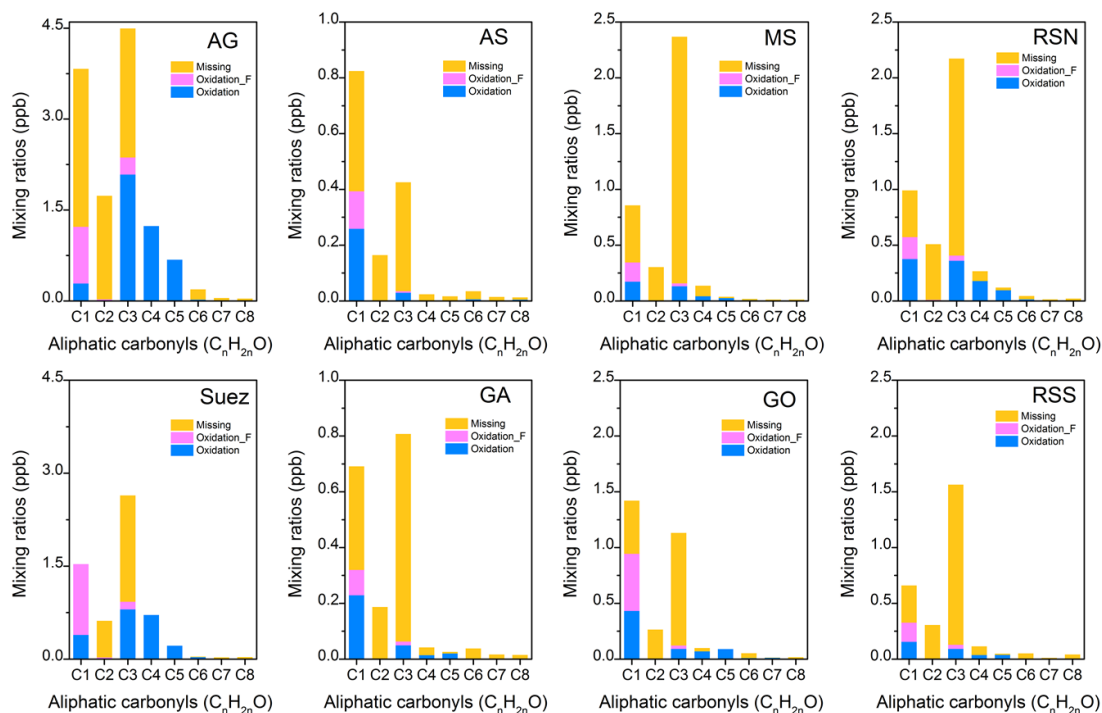
315 where X and Y refer to two hydrocarbon compounds with different rates of reaction with the OH radical (k). For this study, we  
316 chose toluene ( $k_{OH+toluene} = 5.63E-12 \text{ cm}^3 \text{ molecule}^{-1}\text{s}^{-1}$ ) and benzene ( $k_{OH+benzene} = 1.22E-12 \text{ cm}^3 \text{ molecule}^{-1}\text{s}^{-1}$ ) (Atkinson and Arey,  
317 2003), because both compounds were measured by PTR-ToF-MS at high frequency and these values showed a good agreement  
318 with values measured by GC-FID (Figure S2). The approach detailed by Yuan et al. (2012) was applied to determine the initial  
319 emission ratio  $\frac{[X]}{[Y]} \Big|_{t=0}$  in each area: MS (1.46), S (2.50), RSN (1.25), RSS (2.50), GA (1.96), AS (1.25), GO (2.50) and AG (1.75).  
320 The corresponding correlation plots of toluene and benzene for each region can be found in Figure S3. An average value of OH  
321 exposure in each area was applied in equation (2) to derive the predicted mixing ratio of each aliphatic carbonyl. There are  
322 limitations and uncertainties in using the hydrocarbon ratios to obtain the photochemical age  $\Delta t$  (OH exposure in this study),  
323 especially in remote area lacking hydrocarbon (benzene and toluene in this case) sources, which would introduce uncertainty to  
324 the initial emission ratio determination (Yuan et al., 2012;Lewis et al., 2005). Nevertheless, it can still provide insights on  
325 photochemical processing (Parrish et al., 2007;McKeen et al., 1996), which will be discussed afterwards.

326 Figure 3 shows the calculated mixing ratios of the aliphatic carbonyls and the unattributed fraction compared with the mean values  
327 of measurements in each area. The calculated carbonyl mixing ratios are sub-divided in the plot to show the fraction stemming  
328 from a parent hydrocarbon with the same carbon number, and the fraction resulting from fragmentation of a hydrocarbon with a  
329 higher carbon number. In general, the direct oxidation fraction varied from area to area for C1 to C3 carbonyls (formaldehyde,  
330 acetaldehyde and acetone). For C4 and C5 carbonyls, the mixing ratios could be fully attributed to the direct oxidation fraction  
331 over the Arabian Gulf and Suez (polluted region with high loadings), while in other regions, direct oxidation fraction could only  
332 partially explain the measured mixing ratios. For C7 and C8 carbonyls, the oxidation fraction generally explained < 20% of  
333 measured mixing ratios. Notably, for acetone, the oxidation (mainly from propane oxidation) contributed much more of the direct  
334 oxidation fraction over the Arabian Gulf (53%) and Suez (35%) than those in other regions (~10%), indicating OH radical initiated  
335 hydrocarbon oxidation (and subsequent secondary photochemical processes) play a more important role in polluted regions than  
336 in other less polluted regions. This is also consistent with the results that showed C4 and C5 carbonyls mixing ratios could be fully  
337 attributed by the direct oxidation fractions. The high-unattributed levels of acetone especially over the remote areas are possibly  
338 due to transportation as its long lifetime from 15 days up to more than two months in the boundary layer (Singh et al., 1994)  
339 compared to the other carbonyl compounds.



340 The distribution for acetaldehyde was markedly different to that of acetone. The measured mixing ratios were mainly determined  
341 by the unattributed fraction, even over the Arabian Gulf and Suez, where the oxidation fraction only accounts for < 5%. Because  
342 the OH rate coefficient for acetaldehyde (at 298 K) is two orders of magnitude larger than that for acetone, long-distance transport  
343 of short-lived acetaldehyde was limited. Although oxidation from unconsidered hydrocarbons could be a reason, the much larger  
344 unattributed fraction compared with that of acetone indicates that OH radical driven oxidation of the main hydrocarbons present  
345 cannot explain the measured acetaldehyde level in this region. This points to the existence of other production pathways (primary  
346 and/or secondary) of acetaldehyde. Therefore, we compared the measured acetaldehyde with the results from a complex  
347 atmospheric chemistry model (EMAC) which includes transport and known sources to further investigate the discrepancy. This  
348 discussion is given in section 3.4 and 3.5.

349 Formaldehyde had a more than 50% contribution from hydrocarbon oxidation over the Red Sea and Gulf of Oman but less than  
350 40% over the Arabian Gulf. Over the Suez region, calculated formaldehyde level was even 24% higher than the measured mean  
351 mixing ratio. The contribution from other hydrocarbons is more significant than from methane oxidation over the Arabian Gulf,  
352 Suez and Gulf of Oman. Atmospheric formaldehyde has been reported as having various primary and secondary sources and,  
353 unlike the other carbonyls, photolysis is an important sink (Carlier et al., 1986). Neither the primary sources nor the photolysis  
354 were considered in the calculation. Therefore, different unattributed fractions in the Arabian Gulf and Suez suggest the existence  
355 of different formaldehyde formation pathways. Similar to acetaldehyde, due to the short lifetime, the unattributed fraction indicates  
356 unconsidered sources and formation pathways.

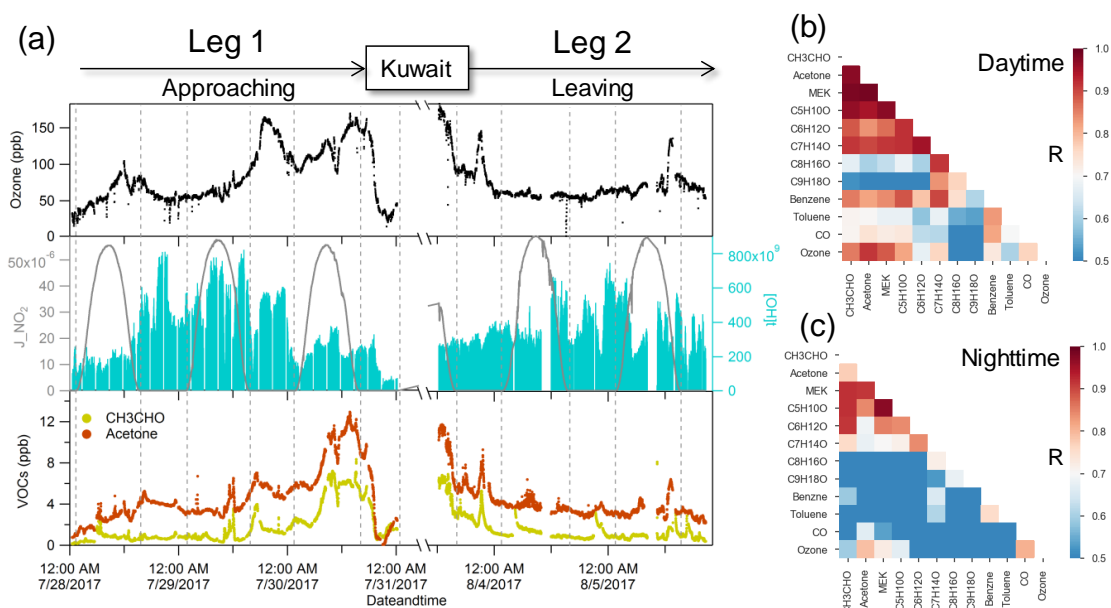


357

358 Figure 3. Measured and calculated aliphatic carbonyls as mentioned in the text for different regions during the AQABA campaign:  
359 Oxidation (in blue) represents aliphatic carbonyls produced from alkane oxidation with the same carbon number; Oxidation\_F  
360 represents aliphatic carbonyls produced from other hydrocarbon oxidation; Missing (in yellow) is the unattributed fraction  
361 compared with the mean values of measurements.

### 362 3.2.2 Case studies: the Arabian Gulf and Suez region

363 The primary emission sources in the Arabian Gulf and Suez regions are quite different. While the Arabian Gulf is dominated by  
364 oil and gas operations, Suez is more influenced by ship emissions and urban areas (Bourtsoukidis et al., 2019). Carbonyl  
365 compounds were most abundant in these two areas. As mentioned before, photochemical oxidation contributed a large fraction to  
366 acetone and the larger aliphatic carbonyls over the Arabian Gulf and Suez areas, but could not explain the high level of acetaldehyde  
367 measured in both regions. For further insight, we focused on a time series of selected trace-gases along with the correlations among  
368 them to better identify the sources of the major aliphatic carbonyls.

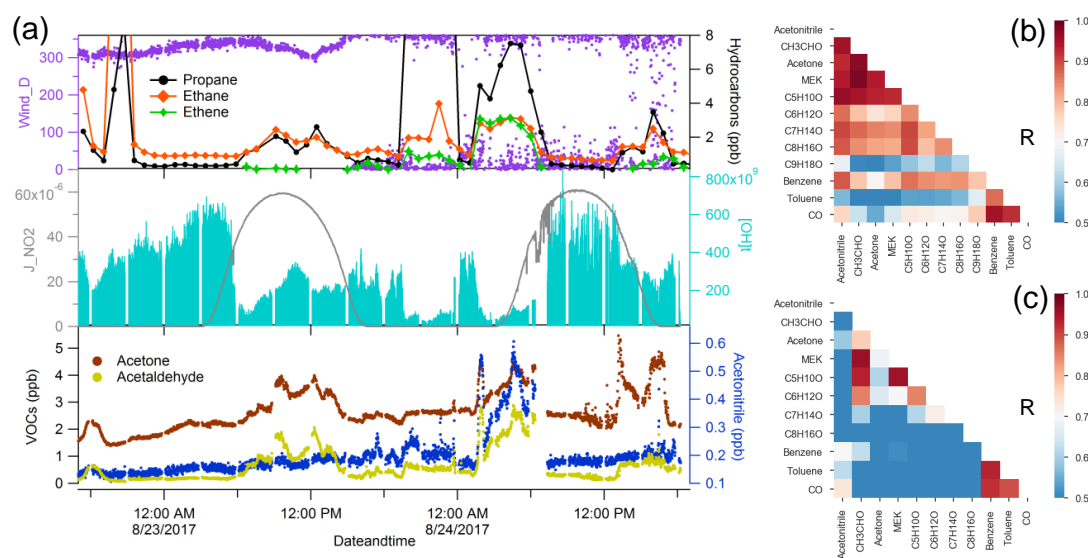


369  
370 Figure 4. Case study of the Arabian Gulf. (a) Time series of selected species measured over the Arabian Gulf; (b) daytime  
371 correlation heat map of selected species; (c) nighttime correlation heat map of selected species.

372 Figure 4(a) shows the time series of acetaldehyde and acetone over the Arabian Gulf along with OH exposure ( $[OH]t$ ) and ozone.  
373 We further separated the data into daytime and nighttime and calculated correlations among the carbonyls and other selected  
374 species (see Fig. 4b and c). Aliphatic carbonyls were well correlated with each other during the daytime and ozone had a generally  
375 good correlation with C<sub>2</sub>-C<sub>7</sub> carbonyls ( $r > 0.7$ ) during the daytime but a much lower correlation during the night, indicating ozone  
376 and carbonyls were co-produced via photochemical oxidation. This further emphasizes the importance of local photochemical  
377 production of aliphatic carbonyls over the Arabian Gulf, as suggested in previous section 3.2.1. Meanwhile, as shown in Figure 4  
378 (a), the calculated OH exposure was high during the first night in leg 1, where an elevation of acetone mixing ratio was observed  
379 while the mixing ratio of acetaldehyde remained relatively constant. With limited OH radical abundance during the nighttime, the  
380 increased OH exposure indicates that the air reaching the ship was photochemically processed (aged). Therefore, the increase of  
381 acetone was mainly from long-distance transport as acetone has a much longer atmospheric lifetime than acetaldehyde. As the ship  
382 approached Kuwait, the calculated OH exposure was low (starting from 7/30/2017, 12:00 am UTC), which is an indicator of nearby  
383 emission sources. The lifetime of the OH radical derived from the measured OH reactivity also decreased from  $\sim 0.1$  s to  $\sim 0.04$  s  
384 during the same period (Pfanterstill et al., 2019). Oil fields and associated refineries are densely distributed in the northwest of the  
385 Arabian Gulf region (United States Central Intelligence Agency). The air reaching the ship when mixing ratios of acetone and



386 acetaldehyde were highest was mainly from the Northwest (Iraq oil field region) according to the back trajectories (Bourtsoukidis  
387 et al., 2019). This suggests that the air masses encountered in Northwest Arabian Gulf were a combination of fresh emissions from  
388 nearby sources and photochemically processed air transported from elsewhere. During the second leg, relatively low mixing ratios  
389 were identified in the same region (Northwest Arabian Gulf), which was mainly due to a greater influence of air masses originating  
390 from less populated desert regions of Northeast Iran (Bourtsoukidis et al., 2019) with much less influence from the oil field  
391 emissions, meaning less precursors were available for carbonyl production. Several plumes (extending over 2-3 hours) of elevated  
392 carbonyls with increased ozone were observed during the nighttime for both legs (Fig. 4a), indicating transport of highly polluted  
393 air.



394

395 Figure 5. Case study of Suez. (a) Time series of selected species measured over Suez; (b) correlation heat map of selected species  
396 during biomass burning plume (UTC 01:00 -06:00 August 24<sup>th</sup> 2017); (c) correlation heat map of selected species without the  
397 period of biomass burning plume.

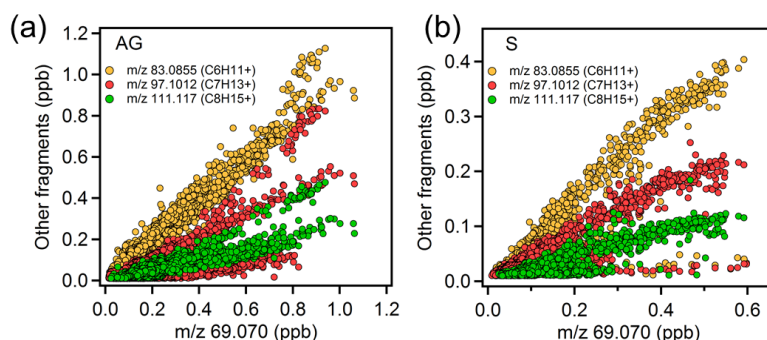
398 For the Suez region (Gulf of Suez and Suez Canal), data were only available for the second leg. A significant increase of acetonitrile  
399 (over 400 ppt) was observed just before entering the Great Bitter Lake (see Figure 5a), indicating an increasing influence of biomass  
400 burning on the air composition (Lobert et al., 1990). Carbonyl compounds are important primary emissions in fresh biomass  
401 burning plumes (Holzinger et al., 1999;Schauer et al., 2001;Holzinger et al., 2001;Koss et al., 2018) as well as being formed as  
402 secondary products in more aged plumes (Holzinger et al., 2005). We further investigated the correlation coefficient among  
403 carbonyls during the biomass burning plume (Figure 5b) in Suez. Carbonyls had a high correlation with acetonitrile, benzene and  
404 among themselves, particularly for smaller carbonyls (acetaldehyde, C3-C5 carbonyls). The biomass burning emissions were  
405 probably transported by on the prevailing northerly wind above Northeast Egypt (southern side of Suez Canal) where crop residues  
406 especially rice straw is often directly burned in the open fields (Abdelhady et al., 2014;Said et al., 2013;Youssef et al., 2009).  
407 Besides the direct biomass burning emission, the high mixing ratios and the good correlations of carbonyls could also have resulted  
408 from other sources as hydrocarbons (alkanes, alkenes and aromatics) which were elevated at the same time. Similar to conditions  
409 identified over the Arabian Gulf, elevated OH exposure accompanied with increasing acetone mixing ratio was observed during  
410 the first night over the Gulf of Suez, indicating aged air mass transportation. The OH exposure was then significantly lower during  
411 the daytime, when mixing ratios of carbonyls and alkanes increased as well. This indicates the presence of emission sources nearby.



412 Oil refineries located in the costal side of Suez and oil tank terminals located in the northern part of the Gulf of Suez are likely  
413 sources.

### 414 3.3 Air chemistry of unsaturated carbonyls

415 Unsaturated carbonyls measured by PTR-MS have been only rarely reported in the atmosphere with the exception of methyl vinyl  
416 ketone and methacrolein (C<sub>4</sub> carbonyls) which are frequently reported as the oxidation products of isoprene (Williams et al., 2001;  
417 Fan and Zhang, 2004; Wennberg et al., 2018). According to the GC-FID measurement, isoprene was below the detection limit for  
418 most of the time during the AQABA cruise with the highest values observed in Suez (10 - 350 ppt). This shows that the AQABA  
419 campaign was little influenced by either terrestrial or marine isoprene emissions. However, we observed unexpected high levels  
420 on mass 69.070, which is usually interpreted as isoprene for PTR-MS measurements. Significant enhancements were even  
421 identified while sampling our own ship exhaust (in PTR-MS but not GC-FID), suggesting the presence of an anthropogenic  
422 interference at that mass under these extremely polluted conditions. Several studies have reported possible fragmentations of cyclic  
423 alkanes giving mass (m/z) 69.070. These include: a laboratory study on gasoline hydrocarbon measurements by PTR-MS  
424 (Gueneron et al., 2015), a GC-PTR-MS study of an oil spill site combined with analysis of crude oil samples (Yuan et al., 2014)  
425 and an inter-comparison of PTR-MS and GC in an O&G industrial site (Warneke et al., 2014). From those studies, other  
426 fragmentations from C<sub>5</sub>-C<sub>9</sub> cycloalkanes including m/z 43, m/z 57, m/z 83, m/z 111 and m/z 125 were identified together with  
427 m/z 69. Cyclic alkanes were directly measured in oil and gas fields (Simpson et al., 2010; Gilman et al., 2013; Li et al., 2017; Aklilu  
428 et al., 2018), vehicle exhaust (Gentner et al., 2012; Erickson et al., 2014), vessel exhaust (Xiao et al., 2018), accounting for a non-  
429 negligible amount of the total VOCs mass depending on the fuel type. Koss et al. (2017) reported enhancement of cyclic alkane  
430 fragment signals and increased levels of unsaturated carbonyls measured by PTR-ToF-MS over O&G region in the US. The  
431 unsaturated carbonyls (C<sub>5</sub>-C<sub>9</sub>) were assigned as oxidation products of cycloalkanes. Therefore, we examined the correlations  
432 between m/z 69.070 and other cycloalkane fragments over the Arabian Gulf and Suez, where anthropogenic primary emissions  
433 were significant. As shown in Figure 6, m/z 83 was the most abundant fragment and it correlated better with m/z 69 than the other  
434 two masses, strongly supporting the presence of C<sub>6</sub> cycloalkanes (methylcyclopentane and cyclohexane). The other two masses  
435 are distributed in two or three clusters, suggesting compositions of different cycloalkanes. M/z 43 and m/z 57 (fragments of C<sub>5</sub>  
436 cycloalkanes) had lower correlations with other fragments (not shown in the graph) as they are also fragments of other higher  
437 hydrocarbons. Thereby we could assign those unsaturated carbonyls as photochemical oxidation products (i.e. cyclic ketones or  
438 aldehydes) from their precursor cycloalkanes.



439

440 Figure 6. Scatter plots of m/z 69.070 and other cycloalkane fragment masses over the (a) Arabian Gulf and (b) Suez region.

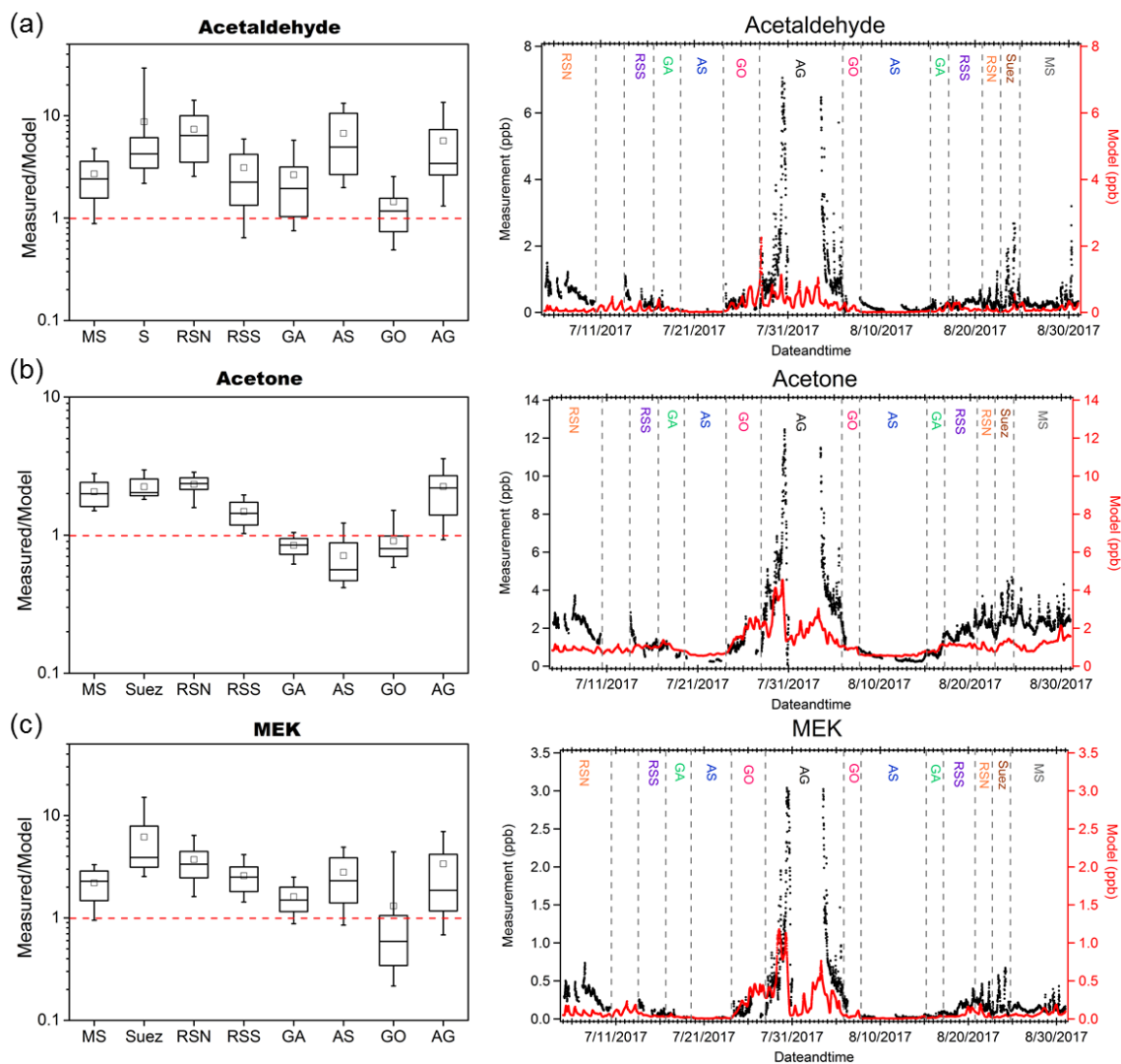


441 As shown in Figure 2 and Table 1, C6 unsaturated carbonyls displayed higher mixing ratios than any other unsaturated carbonyls  
442 over the Arabian Gulf while C5 unsaturated carbonyl was slightly higher than C6 in Suez. Bourtsoukidis et al. (2019) derived  
443 enhancement ratio slopes from pentane isomers and established that the Arabian Gulf is dominated by oil and gas operations and  
444 that Suez is more influenced by ship emissions. Therefore, as the Arabian Gulf had much more active O&G activities than Suez,  
445 our findings agree with Koss et al. (2017) who showed that C6 unsaturated carbonyls should be more abundant than C5 carbonyls  
446 since more precursors for C6 unsaturated carbonyls are emitted from active oil fields. It is worth mentioning that in Figure 6 (b)  
447 one cluster at the bottom showed  $m/z$  69.070 had no correlation with other three masses. Those points correspond to the time when  
448 the GC measured significant elevated isoprene while passing through the narrow Suez Canal where some vegetation (e.g. palms  
449 and some agriculture) was present close to shore, meaning  $m/z$  69.070 during this period was isoprene. At the same time,  $m/z$   
450 71.049 (C4 unsaturated carbonyl) increased from 20 ppt to 220 ppt. Isoprene oxidation products (MVK and methacrolein) were  
451 probably the major contribution to the C4 unsaturated carbonyls in this period. This also explains why C4 carbonyl dominated the  
452 distribution of unsaturated carbonyls over Suez.

453 In the other regions (especially more remote areas), the cyclic alkane fragmentation masses had much lower abundance, leading  
454 to much less unsaturated carbonyls due to lack of precursors. Meanwhile,  $m/z$  69.070 ( $C_5H_8H^+$ ),  $m/z$  83.086 ( $C_6H_{10}H^+$ ) and  $m/z$   
455 97.101 ( $C_7H_{12}H^+$ ) could also be fragmentations from corresponding aldehydes losing one water molecule as mentioned in section  
456 2.3.3. Missing information of the chemical structure of unsaturated carbonyls and knowledge of their precursors, preclude detailed  
457 investigation of the sources of large unsaturated carbonyls in these areas.

### 458 3.4 Model comparison of acetaldehyde, acetone and MEK

459 We compared our measurement results of acetaldehyde, acetone and MEK to those predicted by the global model “EMAC”  
460 (ECHAM5/MESSy2 for Atmospheric Chemistry). The model considers direct emissions (such as anthropogenic, biogenic,  
461 biomass burning etc.), atmospheric transport and mixing, photochemical production of carbonyls (by OH,  $O_3$  and  $NO_3$ ), and  
462 physical and chemical removal processes. From the results shown in Figure 7, the model predicted acetone much better than  
463 acetaldehyde and MEK. In general, the model broadly captured the major features identified during the campaign such as much  
464 higher levels of carbonyls mixing ratios over the Arabian Gulf and Suez and relatively low levels over the Arabian Sea. The mean  
465 measurements-to-model ratios indicated that acetone was overestimated by a factor within 1.5 over the Arabian Sea, Gulf of Aden  
466 and Gulf of Oman, and underestimated by a factor within 2.5 over the other regions. In contrast, the model underestimated MEK  
467 within a factor of 4 over most of the regions except for the Gulf of Oman where MEK was overestimated (median values were  
468 taken here as the mean values substantially deviated from the medians over Suez, Gulf of Oman and Arabian Gulf). The model  
469 underestimation was most significant for acetaldehyde, which is underpredicted by a factor (median values) of more than 6 over  
470 the Red Sea North, ~ 4 over the Arabian Sea and Arabian Gulf and between 1 and 4 over other regions. A strong natural non-  
471 methane hydrocarbon source from deep water in the Northern Red Sea was implemented in the model (Bourtsoukidis et al., 2020).  
472 Although the model representation of acetaldehyde and other carbonyls was clearly improved after including the deep water source  
473 of ethane and propane (Figure S4), the underestimation of acetaldehyde was still significant over the Red Sea North as shown in  
474 Figure 7(a), indicating further missing sources. For acetaldehyde and MEK, the discrepancy was also significant over the Arabian  
475 Sea where acetone was in contrast, overestimated. Since acetaldehyde had the biggest bias from the model prediction both with  
476 our simple empirical calculation (section 3.2.1) and the global model, we further investigate the possible missing sources of  
477 acetaldehyde.



478

479 Figure 7. Measurement to model ratios (left) and time series (right) of measurements (in black) and model simulation (in red) of  
480 (a) acetaldehyde; (b) acetone; (c) MEK in each area. In each box plot, the box represents 25% to 75% of the data set with central  
481 line and square indicating the median value and the mean value respectively. The whiskers show data from 10% to 90%. The red  
482 dashed lines represent the 1:1 ratio.

### 483 3.5 Missing sources of acetaldehyde

484 In this section we investigate the following processes as potential sources of acetaldehyde: (1) production as an inlet artifact, (2)  
485 oceanic emission of acetaldehyde, (3) anthropogenic primary sources, (4) biomass burning sources, and (5) other possible  
486 secondary formation pathways.

#### 487 3.5.1 Inlet artifact

488 Northway et al. (2004) and Apel et al. (2008) reported that heterogeneous reactions of unsaturated organic species with ozone on  
489 the wall of the Teflon inlet can cause artifacts signal of acetaldehyde but not to acetone. During AQABA, the highest and the most



490 variable ozone mixing ratios were observed during the campaign over the Arabian Gulf (mean:  $80 \pm 34$  ppb) and the Red Sea North  
491 ( $66 \pm 12$  ppb), where a modest correlation was found between acetaldehyde and ozone over the Arabian Gulf ( $r^2=0.54$ ) and no  
492 significant correlation over the Red Sea North ( $r^2=0.40$ ). However larger correlation coefficients were identified between ozone  
493 and other carbonyls over the Arabian Gulf (see Figure S5), which suggests that the correlation was due to atmospheric  
494 photochemical production rather than artifacts. Moreover, acetaldehyde was found to have a much worse correlation with ozone  
495 during the nighttime compared to the correlation during the daytime over the Arabian Gulf (Figure 4b and c), which also indicates  
496 that inlet generation of acetaldehyde was insignificant. Over other regions, especially the remote area (the Arabian Sea and Gulf  
497 of Aden), ozone was relatively constant and low, with poor correlation with acetaldehyde mixing ratios. Although we cannot  
498 completely exclude the possible existence of artifacts, the interference is likely to be insignificant in this dataset.

### 499 3.5.2 Oceanic emission

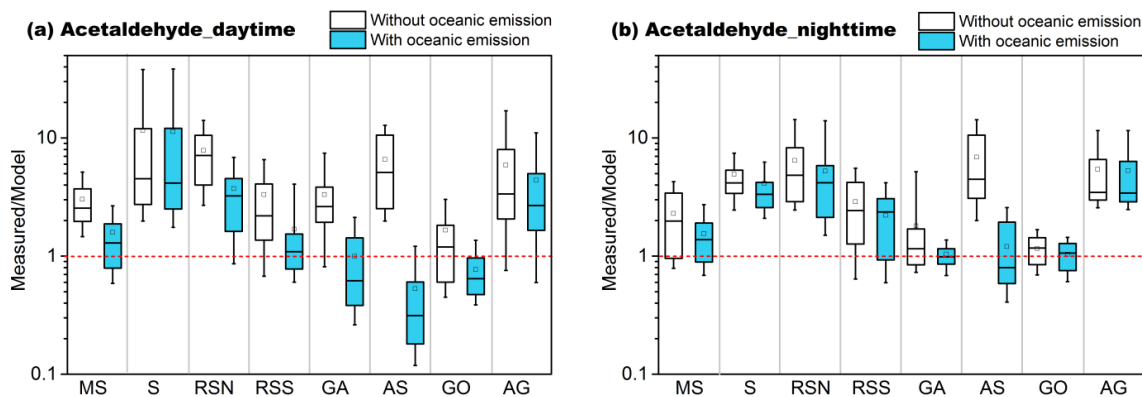
500 A bias between measured acetaldehyde and global model simulations has been observed in previous studies conducted in the  
501 remote troposphere (Singh et al., 2003; Singh, 2004; Wang et al., 2019) and in the marine boundary layer (Read et al., 2012). The  
502 aforementioned studies emphasized the potential importance of the sea water acting as a source of acetaldehyde emission via air-  
503 sea exchange. No significant correlation was found between acetaldehyde and DMS, a marker of marine biogenic emission which  
504 is produced by phytoplankton in seawater (Bates et al., 1992) (see Figure S6). This indicates that the source of acetaldehyde was  
505 probably not from direct biogenic production, which has been reported by Mungall et al. (2017). More likely, acetaldehyde and  
506 other small carbonyl compounds can be formed in the sea especially in the surface microlayer (SML) via photodegradation of  
507 colored dissolved organic matter (CDOM) (Kieber et al., 1990; Zhou and Mopper, 1997; Ciuraru et al., 2015). Zhou and Mopper  
508 (1997) calculated the exchange direction of small carbonyls based on measurement results and identified that the net flux of  
509 acetaldehyde was from sea to the air whereas formaldehyde was taken up by the sea. Sinha et al. (2007) characterized air-sea flux  
510 of several VOCs in a mesocosm experiment and found that acetaldehyde emissions were in close correlation with light intensity  
511 ( $r=0.7$ ). By using a 3-D model, Millet et al. (2010) estimated the net oceanic emission of acetaldehyde to be as high as  $57 \text{ Tg a}^{-1}$   
512 (in a global total budget:  $213 \text{ Tg a}^{-1}$ ), being the second largest global source. A similar approach was applied in a recent study done  
513 by Wang et al. (2019), reporting the upper limit of the net ocean emission of acetaldehyde to be  $34 \text{ Tg a}^{-1}$ . To our knowledge, there  
514 is no clear experimental evidence showing the ocean to be a sink for acetaldehyde.

515 In order to test the importance of the oceanic emission of acetaldehyde, we implemented this source in EMAC model. The measured  
516 sea water concentration of acetaldehyde was not available for the water area around the Arabian Peninsula. Wang et al. (2019)  
517 estimated the global average acetaldehyde surface seawater concentrations of the ocean mixed layer using a satellite-based  
518 approach similar to Millet et al. (2010), where the model estimation agreed well with limited reported measurements. From the  
519 Wang et al. (2019) results, the averaged seawater concentration of acetaldehyde around Arabian Peninsula was generally much  
520 higher from June to August. As the photodegradation of CDOM is highly dependent on sunlight, the air-sea submodel (Pozzer et  
521 al., 2006) was augmented to include throughout the campaign a scaled acetaldehyde seawater concentration in the range of 0 ~ 50  
522 nM according to the solar radiation (Figure S7). With this approach, the average of acetaldehyde seawater concentration estimated  
523 by the model is 13.4 nM, a reasonable level compared to predicted level by Wang et al. (2019).

524 After adding the oceanic source of acetaldehyde, the model estimation was significantly improved (Figure 8). As the oceanic source  
525 in the model is scaled according to the solar radiation, the measurement-to-model ratios were more strongly reduced during the  
526 day compared to the night. With oceanic emission included, the model underestimation was less significant, within a factor of 3  
527 during the day and 4 during the night over the Mediterranean Sea, Red Sea and Gulf of Aden. The most significant improvement  
528 was identified over the Red Sea North. As shown in Figure 9, the model had much better agreement with the measurement after

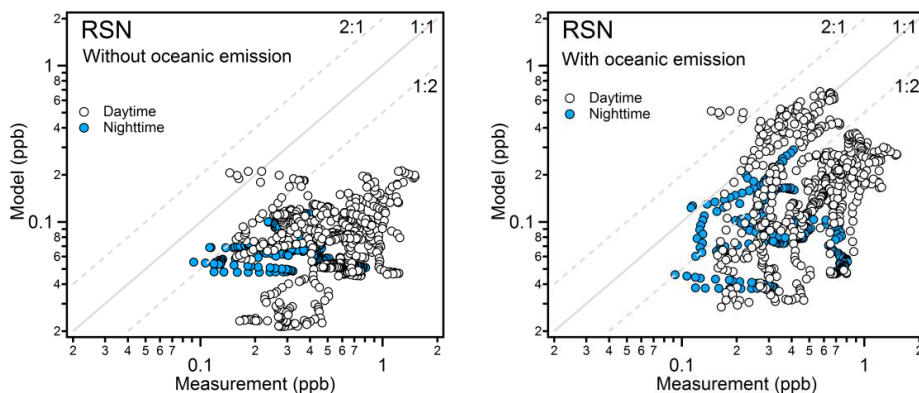
529 adding the oceanic source. The scatter plots for other regions can be found in Figure S8. Over the Arabian Sea, the model  
530 significantly overestimated acetaldehyde mixing ratios, indicating the input sea water concentration of acetaldehyde might be too  
531 high. The SML layer starts to be effectively destroyed by the wave breaking when the wind speed exceeds than  $8 \text{ m s}^{-1}$  (Gantt et  
532 al., 2011). As the average wind speed over the Arabian Sea was the highest among the cruised areas ( $8.1 \pm 2.4 \text{ m s}^{-1}$ , Figure S1),  
533 less contribution from the CDOM photo degradation to acetaldehyde in the surface sea water would be expected. For the Suez  
534 region, due to the limited model resolution ( $1.1^\circ \times 1.1^\circ$ ), little sea water was identified in the model, leading to negligible influence  
535 from the oceanic source.

536 Model underestimation of acetaldehyde especially over the Suez, Red Sea and Arabian Gulf is also likely to be related to the coarse  
537 model resolution ( $\sim 1.1^\circ \times 1.1^\circ$ ) (Fischer et al., 2015). Where model grid points contain areas of land the higher and more variable  
538 terrestrial boundary layer height impacts the model prediction whereas the measurements may only by influenced by a shallower  
539 and more stable marine boundary layer.



540

541 Figure 8. Acetaldehyde measurement to model ratios without the oceanic source (white boxes) and with the oceanic source (blue  
542 boxes) in the model during (a) daytime and (b) nighttime in different regions. The boxes represent 25% to 75% of the data set  
543 with the central line and square indicating the median and mean values, respectively. The whiskers show data from 10% to 90%.  
544 The red dashed lines represent the 1:1 ratio.



545

546 Figure 9. Observed and simulated mixing ratios of acetaldehyde over the Red Sea North without oceanic emission (left) and with  
547 oceanic emission (right). The data points are separated into day- and nighttime according to solar radiation.

548





### 549 3.5.3 Anthropogenic primary sources

550 Over the Arabian Gulf and Suez, the intensive photochemical production of carbonyls is apparent. Therefore, an underestimation  
551 of the precursor hydrocarbons especially those large alkanes, alkenes and cyclic hydrocarbons which were not measured ( $> C_{12}$ )  
552 or included in the model ( $> C_5$ ) could be a reason for the model underestimation of acetaldehyde and other carbonyls. Bourtsoukidis  
553 et al. (2020) compared measured hydrocarbons (ethane, propane, ethene etc.) with the results from model simulations (the same  
554 model used in this study) and periodically found significant model underestimations in both regions. This indicates that not all  
555 sources were present in the model's emission inventory. As mentioned in the previous case studies, high ozone mixing ratios were  
556 observed over the Arabian Gulf and Suez. With large amounts of alkenes present in those regions, which the model occasionally  
557 underestimated, the nighttime ozonolysis of alkenes could be another important source for acetaldehyde, formaldehyde and other  
558 carbonyls (Atkinson et al., 1995; Altshuller, 1993). Acetaldehyde, an oxygenated VOC, is not generally considered as an important  
559 primary emission from oil and gas field but instead a photochemical product of hydrocarbon oxidation (Yuan et al., 2014; Koss et  
560 al., 2015; Koss et al., 2017). In contrast, primary sources of formaldehyde from oil and gas production processes including both  
561 combustion and non-combustion process have been ascertained (Vaught, 1991). Le Baron and Stoeckenius (2015) concluded in  
562 their report of the Uinta Basin winter ozone study that besides formaldehyde, the other carbonyls were poorly understood in terms  
563 of their primary sources. Acetaldehyde and other carbonyls (aldehydes and ketones) have been reported as primary emissions from  
564 fossil fuel combustion including ship emissions (Reda et al., 2014; Xiao et al., 2018; Huang et al., 2018) and vehicle emissions  
565 (Nogueira et al., 2014; Erickson et al., 2014; Dong et al., 2014). Therefore, the active petroleum industry located in the Arabian  
566 Gulf and intensive marine transportation in Suez are likely primary sources of acetaldehyde and other carbonyls which were not  
567 well constrained in the model. The Suez region, where the largest acetaldehyde discrepancy was identified, had a significant  
568 influence from biomass burning (see section 3.2.2). Biomass burning emissions are notoriously difficult to model as they are highly  
569 variable both in time and space. In this study, the model failed to reproduce the acetonitrile level with a range of only 40-50 ppt  
570 rather than 100-550 ppt measured over Suez. Thus, besides the possibility of seawater emission from the Gulf of Suez and the Suez  
571 Canal, the underestimated biomass burning source in the model over Suez, will lead to an underestimation of acetaldehyde as well  
572 as other carbonyl compounds in this region.

### 573 3.5.4 Other possible secondary formation pathways

574 Although the model estimation was generally improved with the addition of an oceanic source, the model to measured ratios still  
575 varied over a wide range. As mentioned above, photodegradation of CDOM on the surface of seawater is a known source for  
576 acetaldehyde although some studies focusing on real sea water samples did not observe clear diel cycles of seawater acetaldehyde  
577 (Beale et al., 2013; Yang et al., 2014). Fast microbial oxidation could be a reason (Dixon et al., 2013) while other non-light driven  
578 sources of acetaldehyde could be an alternative explanation. In a recent study, Zhou et al. (2014) reported enhanced gas-phase  
579 carbonyl compounds including acetaldehyde during a laboratory experiment of ozone reacting with SML samples, indicating  
580 acetaldehyde could also be produced under non-light driven heterogeneous oxidation. Wang et al. (2019) ventured a hypothetical  
581 source that organic aerosol can be an extra source for unattributed acetaldehyde in the free troposphere through light-driven  
582 production and ozonolysis. However, since the yield of acetaldehyde from such reactions is unknown, large uncertainties remain.  
583 Previous studies have shown that the organic matter fraction was highest in smaller sea spray aerosols and that the aerosols contain  
584 both saturated and unsaturated fatty acids originating from the seawater surface (i.e. SML) (Mochida et al., 2002; Cochran et al.,  
585 2016). Thus, for the AQABA campaign, both photodegradation and heterogeneous oxidation could occur on the surface of sea  
586 spray and pollution associated aerosols, even over remote open ocean therefore being an extra source of acetaldehyde and other  
587 carbonyl compounds. Another acetaldehyde formation pathway reported is gas-phase photolysis of pyruvic acid (Eger et al.,



588 2019b; Reed Harris et al., 2016), a compound mainly of biogenic origin. Pyruvic acid has been also observed in seawater (Kieber  
589 and Mopper, 1987; Zhou and Mopper, 1997; Tedetti et al., 2006), although acetaldehyde was not the major product of aqueous-  
590 phase photolysis of pyruvic acid (Griffith et al., 2013). Zhou and Mopper (1997) pointed out that the net exchange direction for  
591 pyruvic acid is expected to be from the air to the sea due to its high partition coefficient (high solubility). Therefore, only low  
592 levels of pyruvic acid would be expected in the remote marine boundary layer. Pyruvic acid was measured by Jardine et al. (2010)  
593 using a PTR-MS at  $m/z$  89 in a forested environment. For the AQABA PTR-ToF-MS data set, enhanced signals were observed at  
594  $m/z$  89.024 with the mean mixing ratio of  $58 \pm 34$  ppt (the box plot can be found in Figure S9), which is much more abundant than  
595 reported pyruvic acid levels measured above Atlantic Ocean ( $1.1 \pm 1.0$  ppt) (Baboukas et al., 2000). This might be due to the  
596 uncertainty associated with the theoretical methods of quantification used here or the presence of isomeric compounds on that  
597 mass, since pyruvic acid was not calibrated with the standard. As the air-sea exchange of pyruvic acid is limited, low levels of  
598 pyruvic acid were expected. Even if we fully assign the  $m/z$  89.024 to pyruvic acid, the contribution to acetaldehyde via photolysis  
599 of pyruvic acid is negligible compared other sources. Therefore, we conclude that the contribution from the photolysis of pyruvic  
600 acid is not an important source for the unattributed acetaldehyde during the AQABA campaign.

#### 601 4 Summary and Conclusion

602 Observations of carbonyl compounds around the Arabian Peninsula were investigated in terms of mixing ratios abundance over  
603 different areas. Aliphatic carbonyl compounds were generally more abundant than the unsaturated and aromatic carbonyl  
604 compounds, and were dominated by low-molecular-weight compounds (carbon number less than five). Aliphatic carbonyl  
605 compounds were found at the highest mixing ratios over the Arabian Gulf followed by the Suez region, while the lowest mixing  
606 ratios were observed over the Arabian Sea and the Gulf of Aden. Over the Mediterranean Sea, aliphatic carbonyls were low except  
607 for acetone that was much higher compared to the levels observed over clean remote areas (i.e. Arabian Sea). The atmospheric  
608 composition over the Red Sea showed obvious differences between the northern and the southern part, with higher mixing ratios  
609 in the north. Similar region-dependent distributions were observed for unsaturated and aromatic carbonyls. Generally, the mixing  
610 ratios of aromatic carbonyl compounds decreased as the carbon number increased. Particularly over the Suez region, benzaldehyde  
611 (C7 aromatic carbonyls) was much more abundant than other aromatic carbonyls, indicating direct sources as well as abundant  
612 oxidation precursors. For unsaturated carbonyl compounds, C5 and C6 carbonyl compounds dominated the mixing ratio  
613 distribution, while the air chemistry highly depends on the chemical structure assignment of those masses.

614 To better understand the air chemistry of aliphatic carbonyl compounds over different regions, we used an empirical method to  
615 calculate the levels of carbonyl compounds resulting from OH oxidation of precursor hydrocarbon species. The results indicate  
616 that mixing ratios of formaldehyde and C3-C8 carbonyl compounds could, to a large part, be explained by OH initiated  
617 photooxidation in each region, especially over the Arabian Gulf and Suez region. This result indicates that photooxidation is a  
618 dominant production pathway for formaldehyde and C3-C8 aliphatic carbonyl compounds in these two regions. However,  
619 acetaldehyde from hydrocarbon precursors was not sufficient to explain the high mixing ratios observed, indicating the existence  
620 of other sources and/or formation pathways. Further case studies showed that the carbonyl compounds produced via photooxidation  
621 were highly correlated to the high ozone levels during daytime over the Arabian Gulf while the air chemistry in Suez region was  
622 strongly influenced by regional biomass burning. Due to the unexpectedly high loading of  $m/z$  69 (usually assigned as isoprene)  
623 observed in highly polluted regions, we further identified the correlations between  $m/z$  69 and other fragmentation masses of  
624 cycloalkanes according to previous studies conducted in oil and gas regions (Warneke et al., 2014; Yuan et al., 2014; Koss et al.,  
625 2017). The high correlations among fragments implied the existence of cycloalkanes in the polluted regions, which could be further  
626 oxidized to unsaturated carbonyl compounds (cyclic ketones or aldehydes).



627 As acetaldehyde was identified as having important additional sources, we further compared the measurements of major carbonyl  
628 species (acetaldehyde, acetone and MEK) with a comprehensive global atmospheric chemistry model (EMAC). Acetaldehyde was  
629 found to have the highest discrepancy between the observations and model simulations, with the simulated values to be lower up  
630 to a factor of 10. By adding an oceanic source of acetaldehyde produced via light-driven photodegradation of CDOM in the  
631 seawater, the model estimation improved significantly, especially over the Red Sea North. With the oceanic source added, modelled  
632 acetaldehyde became slightly overestimated in clean regions, suggesting that the emission rate employed represents an upper limit.  
633 The results indicate that the ocean plays an important role in the atmospheric acetaldehyde budget, under both clean and polluted  
634 conditions. The underestimated acetaldehyde in the model is significant as it will influence the atmospheric budget of e.g. PAN.  
635 As shown in Figure 1, multiple sources and formation pathways need to be considered to better understand the atmospheric budget  
636 of acetaldehyde. Additional laboratory experiments and field measurements are necessary in order to verify all possible  
637 atmospheric formation mechanisms and to improve model simulations.

638

#### 639 **Data availability.**

640 Data will be made available via: <https://edmond.mpdl.mpg.de/imeji/>

#### 641 **Author contributions.**

642 AE and CS performed PTR-ToF-MS measurement and preliminary data processing. NW conducted data analysis and drafted the  
643 article. AP performed EMAC model simulation. EB and LE are responsible for NMHC measurements and data. DD, BH and HF  
644 provided formaldehyde data. Ozone and actinic flux data were contributed by JS and JNC. Methane and carbon monoxide data  
645 were provided by JP. JL designed and realized the campaign. JW supervised the study. All authors contributed to editing the draft  
646 and approved the submitted version.

#### 647 **Competing interest.**

648 The authors declare that they have no conflict of interest.

#### 649 **Acknowledgements**

650 We acknowledge the collaboration with the King Abdullah University of Science and Technology (KAUST), the Kuwait Institute  
651 for Scientific Research (KISR) and the Cyprus Institute (CyI) to fulfill the campaign. We would like to thank Captain Pavel Kirzner  
652 and the crew for their full support on-board the Kommandor Iona, Hays Ships Ltd,. We are grateful for the support from all  
653 members involved in AQABA campaign, especially Dr. Hartwig Harder for his general organization onboard of the campaign;  
654 and Dr. Marcel Dorf, Claus Koepfel, Thomas Klüpfel and Rolf Hofmann for logistical organization and their help with preparation  
655 and setup. We would like to express our gratitude to Ivan Tadic and Philipp Eger for the use of ship exhaust contamination flag.  
656 Nijing Wang would acknowledges the European Union's Horizon 2020 research and innovation programme under the Marie  
657 Skłodowska-Curie grant agreement No. 674911.

658

659

660



## 661 References

- 662 Abdelhady, S., Borello, D., Shaban, A., and Rispoli, F.: Viability Study of Biomass Power Plant Fired with Rice Straw in Egypt,  
663 Energy Procedia, 61, 211-215, <https://doi.org/10.1016/j.egypro.2014.11.1072>, 2014.
- 664 Akilu, Y.-a., Cho, S., Zhang, Q., and Taylor, E.: Source apportionment of volatile organic compounds measured near a cold  
665 heavy oil production area, Atmospheric Research, 206, 75-86, <https://doi.org/10.1016/j.atmosres.2018.02.007>, 2018.
- 666 Altshuler, A. P.: Production of aldehydes as primary emissions and from secondary atmospheric reactions of alkenes and  
667 alkanes during the night and early morning hours, Atmospheric Environment. Part A. General Topics, 27, 21-32,  
668 [https://doi.org/10.1016/0960-1686\(93\)90067-9](https://doi.org/10.1016/0960-1686(93)90067-9), 1993.
- 669 Apel, E. C., Brauers, T., Koppmann, R., Bandowe, B., Boßmeyer, J., Holzke, C., Tillmann, R., Wahner, A., Wegener, R.,  
670 Brunner, A., Jocher, M., Ruuskanen, T., Spirig, C., Steigner, D., Steinbrecher, R., Gomez Alvarez, E., Müller, K., Burrows, J. P.,  
671 Schade, G., Solomon, S. J., Ladstätter-Weißemayer, A., Simmonds, P., Young, D., Hopkins, J. R., Lewis, A. C., Legreid, G.,  
672 Reimann, S., Hansel, A., Wisthaler, A., Blake, R. S., Ellis, A. M., Monks, P. S., and Wyche, K. P.: Intercomparison of  
673 oxygenated volatile organic compound measurements at the SAPHIR atmosphere simulation chamber, Journal of Geophysical  
674 Research, 113, 10.1029/2008jd009865, 2008.
- 675 Atkinson, R., Tuazon, E. C., and Aschmann, S. M.: Products of the Gas-Phase Reactions of a Series of 1-Alkenes and 1-  
676 Methylcyclohexene with the OH Radical in the Presence of NO, Environmental Science & Technology, 29, 1674-1680,  
677 10.1021/es00006a035, 1995.
- 678 Atkinson, R., and Arey, J.: Atmospheric Degradation of Volatile Organic Compounds, Chemical Reviews, 103, 4605-4638,  
679 10.1021/cr0206420, 2003.
- 680 Baboukas, E. D., Kanakidou, M., and Mihalopoulos, N.: Carboxylic acids in gas and particulate phase above the Atlantic Ocean,  
681 Journal of Geophysical Research: Atmospheres, 105, 14459-14471, 10.1029/1999jd900977, 2000.
- 682 Bates, T. S., Lamb, B. K., Guenther, A., Dignon, J., and Stoiber, R. E.: Sulfur emissions to the atmosphere from natural sources,  
683 Journal of Atmospheric Chemistry, 14, 315-337, 10.1007/bf00115242, 1992.
- 684 Beale, R., Dixon, J. L., Arnold, S. R., Liss, P. S., and Nightingale, P. D.: Methanol, acetaldehyde, and acetone in the surface  
685 waters of the Atlantic Ocean, Journal of Geophysical Research: Oceans, 118, 5412-5425, 10.1002/jgrc.20322, 2013.
- 686 Bourtsoukidis, E., Williams, J., Kesselmeier, J., Jacobi, S., and Bonn, B.: From emissions to ambient mixing ratios: online  
687 seasonal field measurements of volatile organic compounds over a Norway spruce-dominated forest in central Germany, Atmos.  
688 Chem. Phys., 14, 6495-6510, <https://doi.org/10.5194/acp-14-6495-2014>, 2014.
- 689 Bourtsoukidis, E., Ernle, L., Crowley, J. N., Lelieveld, J., Paris, J.-D., Pozzer, A., Walter, D., and Williams, J.: Non-methane  
690 hydrocarbon (C2-C8) sources and sinks around the Arabian Peninsula, Atmospheric Chemistry and Physics, 19, 7209-7232,  
691 10.5194/acp-19-7209-2019, 2019.
- 692 Bourtsoukidis, E., Pozzer, A., Sattler, T., Matthaios, V. N., Ernle, L., Edtbauer, A., Fischer, H., Konemann, T., Osipov, S., Paris,  
693 J. D., Pfannerstill, E. Y., Stonner, C., Tadic, I., Walter, D., Wang, N., Lelieveld, J., and Williams, J.: The Red Sea Deep Water is  
694 a potent source of atmospheric ethane and propane, Nat Commun, 11, 447, 10.1038/s41467-020-14375-0, 2020.
- 695 Brilli, F., Gioli, B., Ciccioli, P., Zona, D., Loreto, F., Janssens, I. A., and Ceulemans, R.: Proton Transfer Reaction Time-of-  
696 Flight Mass Spectrometric (PTR-TOF-MS) determination of volatile organic compounds (VOCs) emitted from a biomass fire  
697 developed under stable nocturnal conditions, Atmospheric Environment, 97, 54-67, 10.1016/j.atmosenv.2014.08.007, 2014.
- 698 Buhr, K., van Ruth, S., and Delahunty, C.: Analysis of volatile flavour compounds by Proton Transfer Reaction-Mass  
699 Spectrometry: fragmentation patterns and discrimination between isobaric and isomeric compounds, International Journal of  
700 Mass Spectrometry, 221, 1-7, [https://doi.org/10.1016/S1387-3806\(02\)00896-5](https://doi.org/10.1016/S1387-3806(02)00896-5), 2002.
- 701 Cabrera-Perez, D., Taraborrelli, D., Sander, R., and Pozzer, A.: Global atmospheric budget of simple monocyclic aromatic  
702 compounds, Atmospheric Chemistry and Physics, 16, 6931-6947, 10.5194/acp-16-6931-2016, 2016.
- 703 Carlier, P., Hannachi, H., and Mouvier, G.: The chemistry of carbonyl compounds in the atmosphere—A review, Atmospheric  
704 Environment (1967), 20, 2079-2099, [https://doi.org/10.1016/0004-6981\(86\)90304-5](https://doi.org/10.1016/0004-6981(86)90304-5), 1986.
- 705 Celik, S., Drewnick, F., Fachinger, F., Brooks, J., Darbyshire, E., Coe, H., Paris, J. D., Eger, P. G., Schuladen, J., Tadic, I.,  
706 Friedrich, N., Dienhart, D., Hottmann, B., Fischer, H., Crowley, J. N., Harder, H., and Borrmann, S.: Influence of vessel  
707 characteristics and atmospheric processes on the gas and particle phase of ship emission plumes: In-situ measurements in the  
708 Mediterranean Sea and around the Arabian Peninsula, Atmos. Chem. Phys. Discuss., 2019, 1-36, 10.5194/acp-2019-859, 2019.
- 709 Ciuraru, R., Fine, L., van Pinxteren, M., D'Anna, B., Herrmann, H., and George, C.: Photosensitized production of functionalized  
710 and unsaturated organic compounds at the air-sea interface, Sci Rep, 5, 12741, 10.1038/srep12741, 2015.



- 711 Cochran, R. E., Laskina, O., Jayarathne, T., Laskin, A., Laskin, J., Lin, P., Sultana, C., Lee, C., Moore, K. A., Cappa, C. D.,  
712 Bertram, T. H., Prather, K. A., Grassian, V. H., and Stone, E. A.: Analysis of Organic Anionic Surfactants in Fine and Coarse  
713 Fractions of Freshly Emitted Sea Spray Aerosol, *Environ Sci Technol*, 50, 2477-2486, 10.1021/acs.est.5b04053, 2016.
- 714 Colomb, A., Williams, J., Crowley, J., Gros, V., Hofmann, R., Salisbury, G., Klüpfel, T., Kormann, R., Stickler, A., Forster, C.,  
715 and Lelieveld, J.: Airborne Measurements of Trace Organic Species in the Upper Troposphere Over Europe: the Impact of Deep  
716 Convection, *Environmental Chemistry*, 3, 244, 10.1071/en06020, 2006.
- 717 Colomb, A., Gros, V., Alvain, S., Sarda-Esteve, R., Bonsang, B., Moulin, C., Klüpfel, T., and Williams, J.: Variation of  
718 atmospheric volatile organic compounds over the Southern Indian Ocean (30 - 49°S), *Environmental Chemistry*, 6, 70,  
719 10.1071/en08072, 2009.
- 720 de Gouw, J., and Warneke, C.: Measurements of volatile organic compounds in the earth's atmosphere using proton-transfer-  
721 reaction mass spectrometry, *Mass Spectrometry Reviews*, 26, 223-257, 2007.
- 722 de Gouw, J. A., Middlebrook, A. M., Warneke, C., Goldan, P. D., Kuster, W. C., Roberts, J. M., Fehsenfeld, F. C., Worsnop, D.  
723 R., Canagaratna, M. R., Pszenny, A. A. P., Keene, W. C., Marchewka, M., Bertman, S. B., and Bates, T. S.: Budget of organic  
724 carbon in a polluted atmosphere: Results from the New England Air Quality Study in 2002, *Journal of Geophysical Research:*  
725 *Atmospheres*, 110, doi:10.1029/2004JD005623, 2005.
- 726 Derstroff, B., Hüser, I., Bourtsoukidis, E., Crowley, J. N., Fischer, H., Gromov, S., Harder, H., Janssen, R. H. H., Kesselmeier,  
727 J., Lelieveld, J., Mallik, C., Martinez, M., Novelli, A., Parchatka, U., Phillips, G. J., Sander, R., Sauvage, C., Schuladen, J.,  
728 Stöner, C., Tomsche, L., and Williams, J.: Volatile organic compounds (VOCs) in photochemically aged air from the eastern  
729 and western Mediterranean, *Atmospheric Chemistry and Physics*, 17, 9547-9566, 10.5194/acp-17-9547-2017, 2017.
- 730 Dixon, J. L., Beale, R., and Nightingale, P. D.: Production of methanol, acetaldehyde, and acetone in the Atlantic Ocean,  
731 *Geophysical Research Letters*, 40, 4700-4705, 10.1002/grl.50922, 2013.
- 732 Dolgorouky, C., Gros, V., Sarda-Esteve, R., Sinha, V., Williams, J., Marchand, N., Sauvage, S., Poulain, L., Sciare, J., and  
733 Bonsang, B.: Total OH reactivity measurements in Paris during the 2010 MEGAPOLI winter campaign, *Atmospheric Chemistry*  
734 *and Physics*, 12, 9593-9612, 10.5194/acp-12-9593-2012, 2012.
- 735 Dong, D., Shao, M., Li, Y., Lu, S., Wang, Y., Ji, Z., and Tang, D.: Carbonyl emissions from heavy-duty diesel vehicle exhaust in  
736 China and the contribution to ozone formation potential, *Journal of Environmental Sciences*, 26, 122-128,  
737 [https://doi.org/10.1016/S1001-0742\(13\)60387-3](https://doi.org/10.1016/S1001-0742(13)60387-3), 2014.
- 738 Edwards, P. M., Brown, S. S., Roberts, J. M., Ahmadov, R., Banta, R. M., deGouw, J. A., Dube, W. P., Field, R. A., Flynn, J. H.,  
739 Gilman, J. B., Graus, M., Helmig, D., Koss, A., Langford, A. O., Lefer, B. L., Lerner, B. M., Li, R., Li, S. M., McKeen, S. A.,  
740 Murphy, S. M., Parrish, D. D., Senff, C. J., Soltis, J., Stutz, J., Sweeney, C., Thompson, C. R., Trainer, M. K., Tsai, C., Veres, P.  
741 R., Washenfelder, R. A., Warneke, C., Wild, R. J., Young, C. J., Yuan, B., and Zamora, R.: High winter ozone pollution from  
742 carbonyl photolysis in an oil and gas basin, *Nature*, 514, 351-354, 10.1038/nature13767, 2014.
- 743 Eger, P. G., Friedrich, N., Schuladen, J., Shenolikar, J., Fischer, H., Tadic, I., Harder, H., Martinez, M., Rohloff, R., Tauer, S.,  
744 Drewnick, F., Fachinger, F., Brooks, J., Darbyshire, E., Sciare, J., Pikridas, M., Lelieveld, J., and Crowley, J. N.: Shipborne  
745 measurements of ClNO<sub>2</sub> in the Mediterranean Sea and around the Arabian Peninsula during summer, *Atmospheric Chemistry*  
746 *and Physics*, 19, 12121-12140, 10.5194/acp-19-12121-2019, 2019a.
- 747 Eger, P. G., Schuladen, J., Sobanski, N., Fischer, H., Karu, E., Williams, J., Riva, M., Zha, Q., Ehn, M., Quéléver, L. L. J.,  
748 Schallhart, S., Lelieveld, J., and Crowley, J. N.: Pyruvic acid in the boreal forest: first measurements and impact on radical  
749 chemistry, *Atmos. Chem. Phys. Discuss.*, 2019, 1-24, 10.5194/acp-2019-768, 2019b.
- 750 Ellis, A. M., and Mayhew, C. A.: Proton transfer reaction mass spectrometry: principles and applications, John Wiley & Sons,  
751 2013.
- 752 Erickson, M. H., Gueneron, M., and Jobson, B. T.: Measuring long chain alkanes in diesel engine exhaust by thermal desorption  
753 PTR-MS, *Atmospheric Measurement Techniques*, 7, 225-239, 10.5194/amt-7-225-2014, 2014.
- 754 Fall, R.: Abundant Oxygenates in the Atmosphere: A Biochemical Perspective, *Chemical Reviews*, 103, 4941-4952,  
755 10.1021/cr0206521, 2003.
- 756 Fan, J., and Zhang, R.: Atmospheric Oxidation Mechanism of Isoprene, *Environmental Chemistry*, 1, 140-149,  
757 <https://doi.org/10.1071/EN04045>, 2004.
- 758 Finlayson-Pitts, B. J., and Pitts, J. N.: Tropospheric Air Pollution: Ozone, Airborne Toxics, Polycyclic Aromatic Hydrocarbons,  
759 and Particles, *Science*, 276, 1045, 10.1126/science.276.5315.1045, 1997.
- 760 Finlayson-Pitts, B. J., and Pitts Jr, J. N.: Chemistry of the upper and lower atmosphere: theory, experiments, and applications,  
761 Elsevier, 1999.





- 762 Fischer, H., Pozzer, A., Schmitt, T., Jöckel, P., Klippel, T., Taraborrelli, D., and Lelieveld, J.: Hydrogen peroxide in the marine  
763 boundary layer over the South Atlantic during the OOMPH cruise in March 2007, *Atmospheric Chemistry and Physics*, 15,  
764 6971-6980, 10.5194/acp-15-6971-2015, 2015.
- 765 Gantt, B., Meskhidze, N., Facchini, M. C., Rinaldi, M., Ceburnis, D., and Dowd, C. D.: Wind speed dependent size-  
766 resolved parameterization for the organic mass fraction of sea spray aerosol, *Atmospheric Chemistry and Physics*, 11, 8777-  
767 8790, 10.5194/acp-11-8777-2011, 2011.
- 768 Gentner, D. R., Isaacman, G., Worton, D. R., Chan, A. W. H., Dallmann, T. R., Davis, L., Liu, S., Day, D. A., Russell, L. M.,  
769 Wilson, K. R., Weber, R., Guha, A., Harley, R. A., and Goldstein, A. H.: Elucidating secondary organic aerosol from diesel and  
770 gasoline vehicles through detailed characterization of organic carbon emissions, *Proceedings of the National Academy of  
771 Sciences*, 109, 18318, 10.1073/pnas.1212272109, 2012.
- 772 Gilman, J. B., Lerner, B. M., Kuster, W. C., and de Gouw, J. A.: Source signature of volatile organic compounds from oil and  
773 natural gas operations in northeastern Colorado, *Environ Sci Technol*, 47, 1297-1305, 10.1021/es304119a, 2013.
- 774 Griffith, E. C., Carpenter, B. K., Shoemaker, R. K., and Vaida, V.: Photochemistry of aqueous pyruvic acid, *Proceedings of the  
775 National Academy of Sciences*, 110, 11714, 10.1073/pnas.1303206110, 2013.
- 776 Gueneron, M., Erickson, M. H., VanderSchelden, G. S., and Jobson, B. T.: PTR-MS fragmentation patterns of gasoline  
777 hydrocarbons, *International Journal of Mass Spectrometry*, 379, 97-109, 10.1016/j.ijms.2015.01.001, 2015.
- 778 Guo, H., Ling, Z. H., Cheung, K., Wang, D. W., Simpson, I. J., and Blake, D. R.: Acetone in the atmosphere of Hong Kong:  
779 Abundance, sources and photochemical precursors, *Atmospheric Environment*, 65, 80-88, 10.1016/j.atmosenv.2012.10.027,  
780 2013.
- 781 Holzinger, R., Warneke, C., Hansel, A., Jordan, A., Lindinger, W., Scharffe, D. H., Schade, G., and Crutzen, P. J.: Biomass  
782 burning as a source of formaldehyde, acetaldehyde, methanol, acetone, acetonitrile, and hydrogen cyanide, *Geophysical  
783 Research Letters*, 26, 1161-1164, 10.1029/1999gl900156, 1999.
- 784 Holzinger, R., Jordan, A., Hansel, A., and Lindinger, W.: Automobile Emissions of Acetonitrile: Assessment of its Contribution  
785 to the Global Source, *Journal of Atmospheric Chemistry*, 38, 187-193, 10.1023/A:1006435723375, 2001.
- 786 Holzinger, R., Williams, J., Salisbury, G., Klüpfel, T., de Reus, M., Traub, M., Crutzen, P. J., and Lelieveld, J.: Oxygenated  
787 compounds in aged biomass burning plumes over the Eastern Mediterranean: evidence for strong secondary production of  
788 methanol and acetone, *Atmos. Chem. Phys.*, 5, 39-46, 10.5194/acp-5-39-2005, 2005.
- 789 Hornbrook, R. S., Hills, A. J., Riemer, D. D., Abdelhamid, A., Flocke, F. M., Hall, S. R., Huey, L. G., Knapp, D. J., Liao, J.,  
790 Mauldin III, R. L., Montzka, D. D., Orlando, J. J., Shepson, P. B., Sive, B., Staebler, R. M., Tanner, D. J., Thompson, C. R.,  
791 Turnipseed, A., Ullmann, K., Weinheimer, A. J., and Apel, E. C.: Arctic springtime observations of volatile organic compounds  
792 during the OASIS-2009 campaign, *Journal of Geophysical Research: Atmospheres*, 121, 9789-9813, 10.1002/2015jd024360,  
793 2016.
- 794 Huang, C., Hu, Q., Wang, H., Qiao, L., Jing, S., Wang, H., Zhou, M., Zhu, S., Ma, Y., Lou, S., Li, L., Tao, S., Li, Y., and Lou,  
795 D.: Emission factors of particulate and gaseous compounds from a large cargo vessel operated under real-world conditions,  
796 *Environ Pollut*, 242, 667-674, 10.1016/j.envpol.2018.07.036, 2018.
- 797 Jacob, D. J., Field, B. D., Jin, E. M., Bey, I., Li, Q., Logan, J. A., Yantosca, R. M., and Singh, H. B.: Atmospheric budget of  
798 acetone, *Journal of Geophysical Research: Atmospheres*, 107, ACH 5-1-ACH 5-17, 10.1029/2001jd000694, 2002.
- 799 Jardine, K. J., Sommer, E. D., Saleska, S. R., Huxman, T. E., Harley, P. C., and Abrell, L.: Gas Phase Measurements of Pyruvic  
800 Acid and Its Volatile Metabolites, *Environmental Science & Technology*, 44, 2454-2460, 10.1021/es903544p, 2010.
- 801 Jenkin, M. E., Saunders, S. M., and Pilling, M. J.: The tropospheric degradation of volatile organic compounds: a protocol for  
802 mechanism development, *Atmospheric Environment*, 31, 81-104, 1997.
- 803 Ji, Y., Zhao, J., Terazono, H., Misawa, K., Levitt, N. P., Li, Y., Lin, Y., Peng, J., Wang, Y., Duan, L., Pan, B., Zhang, F., Feng,  
804 X., An, T., Marrero-Ortiz, W., Secrest, J., Zhang, A. L., Shibuya, K., Molina, M. J., and Zhang, R.: Reassessing the atmospheric  
805 oxidation mechanism of toluene, *Proceedings of the National Academy of Sciences*, 114, 8169, 10.1073/pnas.1705463114, 2017.
- 806 Jordan, C., Fitz, E., Hagan, T., Sive, B., Frinak, E., Haase, K., Cottrell, L., Buckley, S., and Talbot, R.: Long-term study of  
807 VOCs measured with PTR-MS at a rural site in New Hampshire with urban influences, *Atmospheric Chemistry and Physics*, 9,  
808 4677-4697, 2009.
- 809 Jöckel, P., Kerkweg, A., Pozzer, A., Sander, R., Tost, H., Riede, H., Baumgaertner, A., Gromov, S., and Kern, B.: Development  
810 cycle 2 of the Modular Earth Submodel System (MESSy2), *Geoscientific Model Development*, 3, 717-752, 10.5194/gmd-3-717-  
811 2010, 2010.





- 812 Khan, M. A. H., Cooke, M. C., Utembe, S. R., Archibald, A. T., Maxwell, P., Morris, W. C., Xiao, P., Derwent, R. G., Jenkin,  
813 M. E., Percival, C. J., Walsh, R. C., Young, T. D. S., Simmonds, P. G., Nickless, G., O'Doherty, S., and Shallcross, D. E.: A  
814 study of global atmospheric budget and distribution of acetone using global atmospheric model STOCHEM-CRI, *Atmospheric*  
815 *Environment*, 112, 269-277, 10.1016/j.atmosenv.2015.04.056, 2015.
- 816 Kieber, D. J., and Mopper, K.: Photochemical formation of glyoxylic and pyruvic acids in seawater, *Marine Chemistry*, 21, 135-  
817 149, [https://doi.org/10.1016/0304-4203\(87\)90034-X](https://doi.org/10.1016/0304-4203(87)90034-X), 1987.
- 818 Kieber, R. J., Zhou, X., and Mopper, K.: Formation of carbonyl compounds from UV-induced photodegradation of humic  
819 substances in natural waters: Fate of riverine carbon in the sea, *Limnology and Oceanography*, 35, 1503-1515,  
820 10.4319/lo.1990.35.7.1503, 1990.
- 821 Kim, K.-H., Hong, Y.-J., Pal, R., Jeon, E.-C., Koo, Y.-S., and Sunwoo, Y.: Investigation of carbonyl compounds in air from  
822 various industrial emission sources, *Chemosphere*, 70, 807-820, <https://doi.org/10.1016/j.chemosphere.2007.07.025>, 2008.
- 823 Koss, A., Yuan, B., Warneke, C., Gilman, J. B., Lerner, B. M., Veres, P. R., Peischl, J., Eilerman, S., Wild, R., Brown, S. S.,  
824 Thompson, C. R., Ryerson, T., Hanisco, T., Wolfe, G. M., Clair, J. M. S., Thayer, M., Keutsch, F. N., Murphy, S., and de Gouw,  
825 J.: Observations of VOC emissions and photochemical products over US oil- and gas-producing regions using high-resolution  
826 H3O+ CIMS (PTR-ToF-MS), *Atmos. Meas. Tech.*, 10, 2941-2968, 10.5194/amt-10-2941-2017, 2017.
- 827 Koss, A. R., de Gouw, J., Warneke, C., Gilman, J. B., Lerner, B. M., Graus, M., Yuan, B., Edwards, P., Brown, S. S., Wild, R.,  
828 Roberts, J. M., Bates, T. S., and Quinn, P. K.: Photochemical aging of volatile organic compounds associated with oil and natural  
829 gas extraction in the Uintah Basin, UT, during a wintertime ozone formation event, *Atmospheric Chemistry and Physics*, 15,  
830 5727-5741, 10.5194/acp-15-5727-2015, 2015.
- 831 Koss, A. R., Sekimoto, K., Gilman, J. B., Selimovic, V., Coggon, M. M., Zarzana, K. J., Yuan, B., Lerner, B. M., Brown, S. S.,  
832 Jimenez, J. L., Krechmer, J., Roberts, J. M., Warneke, C., Yokelson, R. J., and de Gouw, J.: Non-methane organic gas emissions  
833 from biomass burning: identification, quantification, and emission factors from PTR-ToF during the FIREX 2016 laboratory  
834 experiment, *Atmospheric Chemistry and Physics*, 18, 3299-3319, 10.5194/acp-18-3299-2018, 2018.
- 835 Kroll, J. H., Ng, N. L., Murphy, S. M., Varutbangkul, V., Flagan, R. C., and Seinfeld, J. H.: Chamber studies of secondary  
836 organic aerosol growth by reactive uptake of simple carbonyl compounds, *Journal of Geophysical Research*, 110,  
837 10.1029/2005jd006004, 2005.
- 838 Lelieveld, J., Gromov, S., Pozzer, A., and Taraborrelli, D.: Global tropospheric hydroxyl distribution, budget and reactivity,  
839 *Atmospheric Chemistry and Physics*, 16, 12477-12493, 10.5194/acp-16-12477-2016, 2016.
- 840 Lewis, A., Hopkins, J., Carpenter, L., Stanton, J., Read, K., and Pilling, M.: Sources and sinks of acetone, methanol, and  
841 acetaldehyde in North Atlantic marine air, *Atmospheric Chemistry and Physics*, 5, 1963-1974, 2005.
- 842 Li, S.-M., Leithead, A., Moussa, S. G., Liggió, J., Moran, M. D., Wang, D., Hayden, K., Darlington, A., Gordon, M., Staebler,  
843 R., Makar, P. A., Stroud, C. A., McLaren, R., Liu, P. S. K., O'Brien, J., Mittermeier, R. L., Zhang, J., Marson, G., Cober, S. G.,  
844 Wolde, M., and Wentzell, J. J. B.: Differences between measured and reported volatile organic compound emissions from oil  
845 sands facilities in Alberta, Canada, *Proceedings of the National Academy of Sciences*, 114, E3756, 10.1073/pnas.1617862114,  
846 2017.
- 847 Lindinger, W., Hansel, A., and Jordan, A.: On-line monitoring of volatile organic compounds at pptv levels by means of proton-  
848 transfer-reaction mass spectrometry (PTR-MS) medical applications, food control and environmental research, *International*  
849 *Journal of Mass Spectrometry and Ion Processes*, 173, 191-241, 1998.
- 850 Lobert, J. M., Scharffe, D. H., Hao, W. M., and Crutzen, P. J.: Importance of biomass burning in the atmospheric budgets of  
851 nitrogen-containing gases, *Nature*, 346, 552-554, 10.1038/346552a0, 1990.
- 852 McKeen, S. A., Liu, S. C., Hsie, E.-Y., Lin, X., Bradshaw, J. D., Smyth, S., Gregory, G. L., and Blake, D. R.: Hydrocarbon ratios  
853 during PEM-WEST A: A model perspective, *Journal of Geophysical Research: Atmospheres*, 101, 2087-2109,  
854 10.1029/95jd02733, 1996.
- 855 Millet, D. B., Guenther, A., Siegel, D. A., Nelson, N. B., Singh, H. B., de Gouw, J. A., Warneke, C., Williams, J., Eerdeken, G.,  
856 and Sinha, V.: Global atmospheric budget of acetaldehyde: 3-D model analysis and constraints from in-situ and satellite  
857 observations, *Atmospheric Chemistry and Physics*, 10, 3405-3425, 2010.
- 858 Mochida, M., Kitamori, Y., Kawamura, K., Nojiri, Y., and Suzuki, K.: Fatty acids in the marine atmosphere: Factors governing  
859 their concentrations and evaluation of organic films on sea-salt particles, *Journal of Geophysical Research: Atmospheres*, 107,  
860 AAC 1-1-AAC 1-10, 10.1029/2001jd001278, 2002.
- 861 Müller, M., Graus, M., Wisthaler, A., Hansel, A., Metzger, A., Dommen, J., and Baltensperger, U.: Analysis of high mass  
862 resolution PTR-TOF mass spectra from 1,3,5-trimethylbenzene (TMB) environmental chamber experiments, *Atmospheric*  
863 *Chemistry and Physics*, 12, 829-843, 10.5194/acp-12-829-2012, 2012.



- 864 Müller, M., Mikoviny, T., Jud, W., D'Anna, B., and Wisthaler, A.: A new software tool for the analysis of high resolution PTR-  
865 TOF mass spectra, *Chemometrics and Intelligent Laboratory Systems*, 127, 158-165, 10.1016/j.chemolab.2013.06.011, 2013.
- 866 Mungall, E. L., Abbatt, J. P. D., Wentzell, J. J. B., Lee, A. K. Y., Thomas, J. L., Blais, M., Gosselin, M., Miller, L. A.,  
867 Papakyriakou, T., Willis, M. D., and Liggitto, J.: Microlayer source of oxygenated volatile organic compounds in the summertime  
868 marine Arctic boundary layer, *Proc Natl Acad Sci U S A*, 114, 6203-6208, 10.1073/pnas.1620571114, 2017
- 869 Nogueira, T., Dominutti, P. A., de Carvalho, L. R. F., Fornaro, A., and Andrade, M. d. F.: Formaldehyde and acetaldehyde  
870 measurements in urban atmosphere impacted by the use of ethanol biofuel: Metropolitan Area of Sao Paulo (MASP), 2012–  
871 2013, *Fuel*, 134, 505-513, 10.1016/j.fuel.2014.05.091, 2014.
- 872 Northway, M. J., de Gouw, J. A., Fahey, D. W., Gao, R. S., Warneke, C., Roberts, J. M., and Flocke, F.: Evaluation of the role of  
873 heterogeneous oxidation of alkenes in the detection of atmospheric acetaldehyde, *Atmospheric Environment*, 38, 6017-6028,  
874 10.1016/j.atmosenv.2004.06.039, 2004.
- 875 Parrish, D. D., Stohl, A., Forster, C., Atlas, E. L., Blake, D. R., Goldan, P. D., Kuster, W. C., and de Gouw, J. A.: Effects of  
876 mixing on evolution of hydrocarbon ratios in the troposphere, *Journal of Geophysical Research*, 112, 10.1029/2006jd007583,  
877 2007.
- 878 Pfannerstill, E. Y., Wang, N., Edtbauer, A., Bourtsoukidis, E., Crowley, J. N., Dienhart, D., Eger, P. G., Ernle, L., Fischer, H.,  
879 Hottmann, B., Paris, J.-D., Stönnner, C., Tadic, I., Walter, D., Lelieveld, J., and Williams, J.: Shipborne measurements of total OH  
880 reactivity around the Arabian Peninsula and its role in ozone chemistry, *Atmospheric Chemistry and Physics*, 19, 11501-11523,  
881 10.5194/acp-19-11501-2019, 2019.
- 882 Pozzer, A., Jöckel, P., Tost, H., Sander, R., Ganzeveld, L., Kerkweg, A., and Lelieveld, J.: Simulating organic species with the  
883 global atmospheric chemistry general circulation model ECHAM5/MESSy1: a comparison of model results with observations,  
884 *Atmos. Chem. Phys.*, 7, 2527-2550, 10.5194/acp-7-2527-2007, 2007.
- 885 Pozzer, A., de Meij, A., Pringle, K. J., Tost, H., Doering, U. M., van Aardenne, J., and Lelieveld, J.: Distributions and regional  
886 budgets of aerosols and their precursors simulated with the EMAC chemistry-climate model, *Atmospheric Chemistry and  
887 Physics*, 12, 961-987, 10.5194/acp-12-961-2012, 2012.
- 888 Read, K. A., Carpenter, L. J., Arnold, S. R., Beale, R., Nightingale, P. D., Hopkins, J. R., Lewis, A. C., Lee, J. D., Mendes, L.,  
889 and Pickering, S. J.: Multiannual observations of acetone, methanol, and acetaldehyde in remote tropical atlantic air: implications  
890 for atmospheric OVOC budgets and oxidative capacity, *Environ Sci Technol*, 46, 11028-11039, 10.1021/es302082p, 2012.
- 891 Reda, A. A., Schnelle-Kreis, J., Orasche, J., Abbaszade, G., Lintemann, J., Arteaga-Salas, J. M., Stengel, B., Rabe, R., Harndorf,  
892 H., Sippula, O., Streibel, T., and Zimmermann, R.: Gas phase carbonyl compounds in ship emissions: Differences between diesel  
893 fuel and heavy fuel oil operation, *Atmospheric Environment*, 94, 467-478, 10.1016/j.atmosenv.2014.05.053, 2014.
- 894 Reed Harris, A. E., Doussin, J.-F., Carpenter, B. K., and Vaida, V.: Gas-Phase Photolysis of Pyruvic Acid: The Effect of  
895 Pressure on Reaction Rates and Products, *The Journal of Physical Chemistry A*, 120, 10123-10133, 10.1021/acs.jpca.6b09058,  
896 2016.
- 897 Roberts, J. M., Fehsenfeld, F. C., Liu, S. C., Bollinger, M. J., Hahn, C., Albritton, D. L., and Sievers, R. E.: Measurements of  
898 aromatic hydrocarbon ratios and NO<sub>x</sub> concentrations in the rural troposphere: Observation of air mass photochemical aging and  
899 NO<sub>x</sub> removal, *Atmospheric Environment (1967)*, 18, 2421-2432, [https://doi.org/10.1016/0004-6981\(84\)90012-X](https://doi.org/10.1016/0004-6981(84)90012-X), 1984.
- 900 Roeckner, E., Brokopf, R., Esch, M., Giorgetta, M., Hagemann, S., Kornblüeh, L., Manzini, E., Schlese, U., and Schulzweida,  
901 U.: Sensitivity of Simulated Climate to Horizontal and Vertical Resolution in the ECHAM5 Atmosphere Model, *Journal of  
902 Climate*, 19, 3771-3791, 10.1175/JCLI3824.1, 2006.
- 903 Sahu, L. K., Tripathi, N., and Yadav, R.: Contribution of biogenic and photochemical sources to ambient VOCs during winter to  
904 summer transition at a semi-arid urban site in India, *Environ Pollut*, 229, 595-606, 10.1016/j.envpol.2017.06.091, 2017.
- 905 Said, N., El-Shatoury, S. A., Díaz, L. F., and Zamorano, M.: Quantitative appraisal of biomass resources and their energy  
906 potential in Egypt, *Renewable and Sustainable Energy Reviews*, 24, 84-91, <https://doi.org/10.1016/j.rser.2013.03.014>, 2013.
- 907 Sander, R., Baumgaertner, A., Cabrera-Perez, D., Frank, F., Gromov, S., Grooß, J.-U., Harder, H., Huijnen, V., Jöckel, P.,  
908 Karydis, V. A., Niemeyer, K. E., Pozzer, A., Riede, H., Schultz, M. G., Taraborrelli, D., and Tauer, S.: The community  
909 atmospheric chemistry box model CAABA/MECCA-4.0, *Geoscientific Model Development*, 12, 1365-1385, 10.5194/gmd-12-  
910 1365-2019, 2019.
- 911 Saunders, S. M., Jenkin, M. E., Derwent, R., and Pilling, M.: Protocol for the development of the Master Chemical Mechanism,  
912 MCM v3 (Part A): tropospheric degradation of non-aromatic volatile organic compounds, *Atmospheric Chemistry and Physics*,  
913 3, 161-180, 2003.



- 914 Schauer, J. J., Kleeman, M. J., Cass, G. R., and Simoneit, B. R. T.: Measurement of Emissions from Air Pollution Sources. 3.  
915 C1–C29 Organic Compounds from Fireplace Combustion of Wood, *Environmental Science & Technology*, 35, 1716–1728,  
916 10.1021/es001331e, 2001.
- 917 Sheng, J., Zhao, D., Ding, D., Li, X., Huang, M., Gao, Y., Quan, J., and Zhang, Q.: Characterizing the level, photochemical  
918 reactivity, emission, and source contribution of the volatile organic compounds based on PTR-TOF-MS during winter haze  
919 period in Beijing, China, *Atmospheric Research*, 212, 54–63, <https://doi.org/10.1016/j.atmosres.2018.05.005>, 2018.
- 920 Simpson, I. J., Blake, N. J., Barletta, B., Diskin, G. S., Fuelberg, H. E., Gorham, K., Huey, L. G., Meinardi, S., Rowland, F. S.,  
921 Vay, S. A., Weinheimer, A. J., Yang, M., and Blake, D. R.: Characterization of trace gases measured over Alberta oil sands  
922 mining operations: 76 speciated C<sub>2</sub>–C<sub>10</sub> volatile organic compounds (VOCs), CO<sub>2</sub>, CH<sub>4</sub>, CO, NO, NO<sub>2</sub>, NO<sub>y</sub>, O<sub>3</sub> and SO<sub>2</sub>,  
923 *Atmos. Chem. Phys.*, 10, 11931–11954, 10.5194/acp-10-11931-2010, 2010.
- 924 Singh, H. B., O'hara, D., Herlth, D., Sachse, W., Blake, D., Bradshaw, J., Kanakidou, M., and Crutzen, P.: Acetone in the  
925 atmosphere: Distribution, sources, and sinks, *Journal of Geophysical Research: Atmospheres*, 99, 1805–1819, 1994.
- 926 Singh, H. B., Tabazadeh, A., Evans, M. J., Field, B. D., Jacob, D. J., Sachse, G., Crawford, J. H., Shetter, R., and Brune, W. H.:  
927 Oxygenated volatile organic chemicals in the oceans: Inferences and implications based on atmospheric observations and air-sea  
928 exchange models, *Geophysical Research Letters*, 30, 10.1029/2003gl017933, 2003.
- 929 Singh, H. B.: Analysis of the atmospheric distribution, sources, and sinks of oxygenated volatile organic chemicals based on  
930 measurements over the Pacific during TRACE-P, *Journal of Geophysical Research*, 109, 10.1029/2003jd003883, 2004.
- 931 Sinha, V., Williams, J., Meyerhöfer, M., Riebesell, U., Paulino, A. I., and Larsen, A.: Air-sea fluxes of methanol, acetone,  
932 acetaldehyde, isoprene and DMS from a Norwegian fjord following a phytoplankton bloom in a mesocosm experiment, *Atmos.*  
933 *Chem. Phys.*, 7, 739–755, 10.5194/acp-7-739-2007, 2007.
- 934 Sjostedt, S. J., Leaitch, W. R., Levasseur, M., Scarratt, M., Michaud, S., Motard-Côté, J., Burkhardt, J. H., and Abbatt, J. P. D.:  
935 Evidence for the uptake of atmospheric acetone and methanol by the Arctic Ocean during late summer DMS-Emission plumes,  
936 *Journal of Geophysical Research: Atmospheres*, 117, n/a–n/a, 10.1029/2011jd017086, 2012.
- 937 Spanel, P., Doren, J., and Smith, D.: A selected ion flow tube study of the reactions of H<sub>3</sub>O<sup>+</sup>, NO<sup>+</sup>, and O<sub>2</sub><sup>+</sup> with saturated and  
938 unsaturated aldehydes and subsequent hydration of the product ions, *International Journal of Mass Spectrometry*, 213, 163–176,  
939 10.1016/S1387-3806(01)00531-0, 2002.
- 940 Stickler, A., Fischer, H., Williams, J., de Reus, M., Sander, R., Lawrence, M. G., Crowley, J. N., and Lelieveld, J.: Influence of  
941 summertime deep convection on formaldehyde in the middle and upper troposphere over Europe, *Journal of Geophysical*  
942 *Research*, 111, 10.1029/2005jd007001, 2006.
- 943 Stoeckenius, T., and McNally, D.: Final report: 2013 Uinta Basin winter ozone study, ENVIRON International Corporation,  
944 Novato, California, 2014.
- 945 Tanimoto, H., Kameyama, S., Iwata, T., Inomata, S., and Omori, Y.: Measurement of air-sea exchange of dimethyl sulfide and  
946 acetone by PTR-MS coupled with gradient flux technique, *Environ Sci Technol*, 48, 526–533, 10.1021/es4032562, 2014.
- 947 Tedetti, M., Kawamura, K., Charrière, B., Chevalier, N., and Sempéré, R.: Determination of Low Molecular Weight  
948 Dicarboxylic and Ketocarboxylic Acids in Seawater Samples, *Analytical Chemistry*, 78, 6012–6018, 10.1021/ac052226w, 2006.
- 949 Vaught, C.: Locating and estimating air emissions from sources of formaldehyde (revised), Midwest Research Inst., Cary, NC  
950 (United States), 1991.
- 951 United States Central Intelligence Agency: Middle East oil and gas, Washington, D.C.: Central Intelligence Agency, available at:  
952 <https://www.loc.gov/item/2007631392/> (last access: 26 November 2019), 2007.
- 953 Wang, S., Hornbrook, R. S., Hills, A., Emmons, L. K., Tilmes, S., Lamarque, J. F., Jimenez, J. L., Campuzano-Jost, P., Nault, B.  
954 A., Crouse, J. D., Wennberg, P. O., Kim, M., Allen, H., Ryerson, T. B., Thompson, C. R., Peischl, J., Moore, F., Nance, D.,  
955 Hall, B., Elkins, J., Tanner, D., Huey, L. G., Hall, S. R., Ullmann, K., Orlando, J. J., Tyndall, G. S., Flocke, F. M., Ray, E.,  
956 Hanisco, T. F., Wolfe, G. M., St. Clair, J., Commane, R., Daube, B., Barletta, B., Blake, D. R., Weinzierl, B., Dollner, M.,  
957 Conley, A., Vitt, F., Wofsy, S. C., Riemer, D. D., and Apel, E. C.: Atmospheric Acetaldehyde: Importance of Air-Sea Exchange  
958 and a Missing Source in the Remote Troposphere, *Geophysical Research Letters*, 10.1029/2019gl082034, 2019.
- 959 Warneke, C., Karl, T., Judmaier, H., Hansel, A., Jordan, A., Lindinger, W., and Crutzen, P. J.: Acetone, methanol, and other  
960 partially oxidized volatile organic emissions from dead plant matter by abiological processes: Significance for atmospheric HOx  
961 chemistry, *Global Biogeochemical Cycles*, 13, 9–17, 10.1029/98GB02428, 1999.
- 962 Warneke, C., and de Gouw, J. A.: Organic trace gas composition of the marine boundary layer over the northwest Indian Ocean  
963 in April 2000, *Atmospheric Environment*, 35, 5923–5933, [https://doi.org/10.1016/S1352-2310\(01\)00384-3](https://doi.org/10.1016/S1352-2310(01)00384-3), 2001.



- 964 Warneke, C., Geiger, F., Edwards, P. M., Dube, W., Pétron, G., Kofler, J., Zahn, A., Brown, S. S., Graus, M., Gilman, J. B.,  
965 Lerner, B. M., Peischl, J., Ryerson, T. B., de Gouw, J. A., and Roberts, J. M.: Volatile organic compound emissions from the oil  
966 and natural gas industry in the Uintah Basin, Utah: oil and gas well pad emissions compared to ambient air composition,  
967 *Atmospheric Chemistry and Physics*, 14, 10977-10988, 10.5194/acp-14-10977-2014, 2014.
- 968 Wennberg, P. O., Bates, K. H., Crouse, J. D., Dodson, L. G., McVay, R. C., Mertens, L. A., Nguyen, T. B., Praske, E.,  
969 Schwantes, R. H., Smarte, M. D., St Clair, J. M., Teng, A. P., Zhang, X., and Seinfeld, J. H.: Gas-Phase Reactions of Isoprene  
970 and Its Major Oxidation Products, *Chemical Reviews*, 118, 3337-3390, 10.1021/acs.chemrev.7b00439, 2018.
- 971 Williams, J., Roberts, J. M., Bertman, S. B., Stroud, C. A., Fehsenfeld, F. C., Baumann, K., Buhr, M. P., Knapp, K., Murphy, P.  
972 C., Nowick, M., and Williams, E. J.: A method for the airborne measurement of PAN, PPN, and MPAN, *Journal of Geophysical*  
973 *Research: Atmospheres*, 105, 28943-28960, 10.1029/2000JD900373, 2000.
- 974 Williams, J., Pöschl, U., Crutzen, P. J., Hansel, A., Holzinger, R., Warneke, C., Lindinger, W., and Lelieveld, J.: An  
975 Atmospheric Chemistry Interpretation of Mass Scans Obtained from a Proton Transfer Mass Spectrometer Flown over the  
976 Tropical Rainforest of Surinam, *Journal of Atmospheric Chemistry*, 38, 133-166, 10.1023/A:1006322701523, 2001.
- 977 Williams, J., Holzinger, R., Gros, V., Xu, X., Atlas, E., and Wallace, D. W. R.: Measurements of organic species in air and  
978 seawater from the tropical Atlantic, *Geophysical Research Letters*, 31, 10.1029/2004gl020012, 2004.
- 979 White, M. L., Russo, R. S., Zhou, Y., Mao, H., Varner, R. K., Ambrose, J., Veres, P., Wingenter, O. W., Haase, K., Stutz, J.,  
980 Talbot, R., and Sive, B. C.: Volatile organic compounds in northern New England marine and continental environments during  
981 the ICARTT 2004 campaign, *Journal of Geophysical Research*, 113, 10.1029/2007jd009161, 2008.
- 982 Wyche, K. P., Monks, P. S., Ellis, A. M., Cordell, R. L., Parker, A. E., Whyte, C., Metzger, A., Dommen, J., Duplissy, J., Prevot,  
983 A. S. H., Baltensperger, U., Rickard, A. R., and Wulfert, F.: Gas phase precursors to anthropogenic secondary organic aerosol:  
984 detailed observations of 1,3,5-trimethylbenzene photooxidation, *Atmos. Chem. Phys.*, 9, 635-665, 10.5194/acp-9-635-2009,  
985 2009.
- 986 Xiao, Q., Li, M., Liu, H., Fu, M., Deng, F., Lv, Z., Man, H., Jin, X., Liu, S., and He, K.: Characteristics of marine shipping  
987 emissions at berth: profiles for particulate matter and volatile organic compounds, *Atmos. Chem. Phys.*, 18, 9527-9545,  
988 10.5194/acp-18-9527-2018, 2018.
- 989 Yang, M., Beale, R., Liss, P., Johnson, M., Blomquist, B., and Nightingale, P.: Air-sea fluxes of oxygenated volatile organic  
990 compounds across the Atlantic Ocean, *Atmospheric Chemistry and Physics*, 14, 7499-7517, 10.5194/acp-14-7499-2014, 2014.
- 991 Yáñez-Serrano, A. M., Nölscher, A. C., Bourtsoukidis, E., Derstroff, B., Zannoni, N., Gros, V., Lanza, M., Brito, J., Noe, S. M.,  
992 House, E., Hewitt, C. N., Langford, B., Nemitz, E., Behrendt, T., Williams, J., Artaxo, P., Andreae, M. O., and Kesselmeier, J.:  
993 Atmospheric mixing ratios of methyl ethyl ketone (2-butanone) in tropical, boreal, temperate and marine environments,  
994 *Atmospheric Chemistry and Physics*, 16, 10965-10984, 2016.
- 995 Youssef, M. A., Wahid, S. S., Mohamed, M. A., and Askalany, A. A.: Experimental study on Egyptian biomass combustion in  
996 circulating fluidized bed, *Applied Energy*, 86, 2644-2650, <https://doi.org/10.1016/j.apenergy.2009.04.021>, 2009.
- 997 Yuan, B., Shao, M., de Gouw, J., Parrish, D. D., Lu, S., Wang, M., Zeng, L., Zhang, Q., Song, Y., Zhang, J., and Hu, M.:  
998 Volatile organic compounds (VOCs) in urban air: How chemistry affects the interpretation of positive matrix factorization  
999 (PMF) analysis, *Journal of Geophysical Research: Atmospheres*, 117, n/a-n/a, 10.1029/2012jd018236, 2012.
- 1000 Yuan, B., Warneke, C., Shao, M., and de Gouw, J. A.: Interpretation of volatile organic compound measurements by proton-  
1001 transfer-reaction mass spectrometry over the deepwater horizon oil spill, *International Journal of Mass Spectrometry*, 358, 43-48,  
1002 10.1016/j.ijms.2013.11.006, 2014.
- 1003 Yuan, B., Koss, A. R., Warneke, C., Coggon, M., Sekimoto, K., and de Gouw, J. A.: Proton-Transfer-Reaction Mass  
1004 Spectrometry: Applications in Atmospheric Sciences, *Chem Rev*, 117, 13187-13229, 10.1021/acs.chemrev.7b00325, 2017.
- 1005 Zhao, J., and Zhang, R.: Proton transfer reaction rate constants between hydronium ion (H<sub>3</sub>O<sup>+</sup>) and volatile organic compounds,  
1006 *Atmospheric Environment*, 38, 2177-2185, 10.1016/j.atmosenv.2004.01.019, 2004.
- 1007 Zhou, S., Gonzalez, L., Leithead, A., Finewax, Z., Thalman, R., Vlasenko, A., Vagle, S., Miller, L. A., Li, S. M., Bureekul, S.,  
1008 Furutani, H., Uematsu, M., Volkamer, R., and Abbatt, J.: Formation of gas-phase carbonyls from heterogeneous oxidation of  
1009 polyunsaturated fatty acids at the air-water interface and of the sea surface microlayer, *Atmospheric Chemistry and Physics*, 14,  
1010 1371-1384, 10.5194/acp-14-1371-2014, 2014.
- 1011 Zhou, X., and Mopper, K.: Photochemical production of low-molecular-weight carbonyl compounds in seawater and surface  
1012 microlayer and their air-sea exchange, *Marine Chemistry*, 56, 201-213, [https://doi.org/10.1016/S0304-4203\(96\)00076-X](https://doi.org/10.1016/S0304-4203(96)00076-X), 1997.